© 2021. Published by The Company of Biologists Ltd | Development (2021) 148, dev194977. doi:10.1242/dev.194977

RESEARCH ARTICLE

Identification of regulatory elements required for *Stra8* expression in fetal ovarian germ cells of the mouse

Chun-Wei Feng[1,2], Guillaume Burnet[1], Cassy M. Spiller[1,2], Fiona Ka Man Cheung[1], Kallayanee Chawengsaksophak[2,3], Peter Koopman[2] and Josephine Bowles[1,2,*]

ABSTRACT

In mice, the entry of germ cells into meiosis crucially depends on the expression of stimulated by retinoic acid gene 8 (*Stra8*). *Stra8* is expressed specifically in pre-meiotic germ cells of females and males, at fetal and postnatal stages, respectively, but the mechanistic details of its spatiotemporal regulation are yet to be defined. In particular, there has been considerable debate regarding whether retinoic acid is required, *in vivo*, to initiate *Stra8* expression in the mouse fetal ovary. We show that the distinctive anterior-to-posterior pattern of *Stra8* initiation, characteristic of germ cells in the fetal ovary, is faithfully recapitulated when 2.9 kb of the *Stra8* promoter is used to drive eGFP expression. Using *in vitro* transfection assays of cutdown and mutant constructs, we identified two functional retinoic acid responsive elements (RAREs) within this 2.9 kb regulatory element. We also show that the transcription factor DMRT1 enhances *Stra8* expression, but only in the presence of RA and the most proximal RARE. Finally, we used CRISPR/Cas9-mediated targeted mutation studies to demonstrate that both RAREs are required for optimal *Stra8* expression levels *in vivo*.

KEY WORDS: Retinoic acid, Stra8, Meiosis, RARE, Germ cell

INTRODUCTION

The germline provides the genetic and epigenetic link between generations. In order to produce haploid germ cells (oocytes and sperm, respectively, for females and males), diploid germ cells must undergo a specialized form of cell division known as meiosis. Meiosis initiates at different life stages in the two sexes: in females, it is initiated in germ cells during fetal development, shortly after gonadal sex determination, whereas, in the male, meiosis is first triggered postnatally, just before puberty. *Stimulated by retinoic acid gene 8* (*Stra8*) is considered to be the crucial master regulator of meiosis in mammals because *Stra8*-null mice of both sexes are infertile due to the inability of germ cells to enter and progress through meiosis (Anderson et al., 2008; Baltus et al., 2006; Mark et al., 2008). Recent studies suggest that STRA8 acts as a transcription factor and regulates the expression of thousands of genes during the initiation of meiosis (Kojima et al., 2019). Despite the importance of timely onset of *Stra8* expression in pre-meiotic cells of both sexes, the details of how it is induced in germ cells at the appropriate time are not yet clear.

The expression of *Stra8* is highly cell-type specific and is temporally controlled, and there is much evidence that the signalling molecule retinoic acid (RA) is involved in inducing its expression (Griswold et al., 2012). *In vivo*, *Stra8* is expressed exclusively in the germline during normal development. In the fetal ovary, *Stra8* transcripts are detected from 12.5 days post coitum (dpc) in pre-meiotic germ cells, and *Stra8* expression follows an anterior to posterior 'wave' running from 12.5 to 16.5 dpc (Bowles et al., 2006; Menke et al., 2003). This 'wave' pattern is also seen in embryonic ovaries of the RA responsive elements (RARE)-lacZ mouse line, which reports RA activity (Bowles et al., 2016, 2006; Rossant et al., 1991). Germ cells of the male fetal testis do not express *Stra8* (Menke et al., 2003); in the male germline *Stra8* is first expressed in mitotic cells of the postnatal testis and then in pre-meiotic spermatogonia throughout life (Oulad-Abdelghani et al., 1996). *In vitro*, only various pluripotent cell lines [embryonic stem (ES), embryonal carcinoma (EC), embryonic germ (EG) and cultured spermatogenic stem cells (SSC)] respond to RA by upregulating *Stra8* (Oulad-Abdelghani et al., 1996; Wang et al., 2016). In other cell lines, and in all somatic cell types, *Stra8* expression appears insensitive to induction by RA, suggesting that the *Stra8* locus is tightly held in an epigenetically 'closed' configuration and/or that crucial co-regulatory factors are not present in such cells. It makes sense that additional mechanisms would be required to regulate sensitivity to RA, in terms of *Stra8* expression, given that RA is widely available during embryonic and adult life. Aberrant expression of *Stra8* has been observed in a somatic cancer (Kuang et al., 2019), perhaps indicative of the importance of stringent silencing of *Stra8* expression.

For mouse *Stra8*, multiple silencing mechanisms have been identified, including promoter methylation, the actions of polycomb repressive complex 1 (PRC1) and class I/II histone deacetylase (HDAC) function. Germ cell-specific deletion of the DNA methylase enzyme DNMT1 revealed that the *Stra8* promoter is normally methylated and repressed for several days after germ cells colonize the fetal gonad (Hargan-Calvopina et al., 2016). Similarly, silencing by PRC1, and specifically by the repressive mark H3K27me3, is required to prevent precocious *Stra8* expression in germ cells of the fetal ovary (Yokobayashi et al., 2013). It has also been demonstrated that interference with class I/II HDAC function, by *in utero* exposure to trichostatin-A (TSA), leads to precocious *Stra8* expression in germ cells of the fetal ovary (Wang and Tilly, 2010). Presumably, germ cells become more RA sensitive than normal, in terms of *Stra8* expression, when epigenetic silencing is lost. Importantly, in none of the above-mentioned scenarios did loss of repressive epigenetic marks lead to ectopic *Stra8* expression and meiotic onset in germ cells resident in the fetal testis, indicating that

[1]School of Biomedical Sciences, The University of Queensland, Brisbane, Queensland 4072, Australia. [2]Institute for Molecular Bioscience, The University of Queensland, Brisbane, Queensland 4072, Australia. [3]Institute of Molecular Genetics of the Czech Academy of Sciences, v.v.i. Vídeňská 1083, 4 14220 Prague, Czech Republic.

*Author for correspondence (jo.bowles@uq.edu.au)

C.-W.F., 0000-0001-9510-1012; G.B., 0000-0003-1086-3267; C.M.S., 0000-0002-1343-8269; F.K.M.C., 0000-0003-3795-2788; K.C., 0000-0001-9401-2122; J.B., 0000-0003-2867-7438

Handling Editor: Haruhiko Koseki
Received 15 July 2020; Accepted 4 February 2021

Development (2021) 148, dev194977. doi:10.1242/dev.194977

these epigenetic mechanisms are permissive, not instructive, in terms of *Stra8* expression. On the other hand, one potential instructive regulator of *Stra8* expression is the transcription factor doublesex and mab-3 related transcription factor 1 (DMRT1). DMRT1 can bind to the *Stra8* promoter and, when *Dmrt1* is ablated, reduced *Stra8* expression is observed in the fetal ovary (Krentz et al., 2011). Furthermore, recent studies have shown that bone morphogenetic protein (BMP) signalling, using the transcriptional regulator ZGLP1 as its effector, can positively impact on *Stra8* expression, among other functions crucial for the oogenic programme, in a mouse primordial germ cell-like (mPGCLC) model (Miyauchi et al., 2017; Nagaoka et al., 2020).

There has been considerable debate over the question of whether RA is required to trigger meiotic onset in the fetal ovary of the mouse. Treatment of gonadal or germ cell cultures with RA, RA receptor (RAR) agonists and RAR antagonists, shows changes in *Stra8* expression that are consistent with the hypothesis that RA induces *Stra8* expression (Bowles et al., 2010, 2006; Koubova et al., 2006; MacLean et al., 2007; Mu et al., 2013; Ohta et al., 2010; Tedesco et al., 2013; Trautmann et al., 2008). Furthermore, deletion of the RA-degrading enzyme CYP26B1 in embryonic testes allows germ cells to ectopically express *Stra8* (Bowles et al., 2006; MacLean et al., 2007). Importantly, *in vivo* studies carried out in rats demonstrated that RA is not just sufficient but also required for normal meiotic onset because, in the absence of the RA precursor vitamin A, ovarian germ cells remained undifferentiated, as judged by their ongoing expression of the pluripotency-associated marker POU5F1 (also known as OCT4, Li and Clagett-Dame, 2009). On the other hand, concerns about the validity of the hypothesis that RA induces meiosis in the fetal ovary were raised when the deletion of two genes encoding RA-synthesising enzymes *Aldh1a2* and *Aldh1a3* was not sufficient to ablate all *Stra8* expression (Kumar et al., 2011). This led to the suggestion that meiotic initiation in germ cells of the fetal ovary is independent of RA. Although we now know that another RA-synthesising enzyme, encoded by *Aldh1a1*, is also present and able to produce RA and induce *Stra8* in the fetal ovary (Bowles et al., 2016), there have been additional recent studies that demonstrate that depletion of RA-producing enzymes, or RARs, does not completely ablate *Stra8* expression, and the controversy continues (Bellutti et al., 2019; Chassot et al., 2020; Kumar et al., 2013; Raverdeau et al., 2012; Vernet et al., 2020).

Hence, despite its crucial role in fertility, we are still very unclear about how *Stra8* is regulated. In addition to the need for *Stra8* to be expressed in a female-specific manner during fetal life, the exact timing of the onset and duration of *Stra8* expression is likely crucial, as is its complete silencing in somatic cells. To provide further information that might help resolve the issue of whether RA signalling is necessary or dispensable for *Stra8* expression, we aimed to identify upstream regulatory elements involved in the endogenous induction of *Stra8* expression in fetal ovarian germ cells. We created a transgenic line in which 2.9 kb of the mouse *Stra8* promoter drives eGFP expression in the characteristic anterior to posterior wave of germ cell-specific expression. We then identified functional RAREs in the 2.9 kb fragment using F9 EC cells as a model for fetal germ cells. Finally, we subtly mutated two RAREs, singly and in tandem, demonstrating substantially diminished *Stra8* expression, *in vivo*.

RESULTS

Computational analysis reveals putative RARE and DMRT1 binding sites in the mouse *Stra8* upstream sequence

RA regulates transcription by acting as a ligand for nuclear RA receptors (RARs), which partner with retinoid X receptors (RXRs) to form heterodimers. Binding of the RA/RAR/RXR complex to RAREs, typically located in regulatory regions upstream of direct target genes, recruits nuclear receptor co-activators or co-repressors, thereby directly activating or repressing transcription of the associated gene (Mark et al., 2006). RAREs are generally direct repeats (DR) of the hexanucleotide sequence [5′-(A/G)G(G/T)TCA-3′] separated by 1 (DR1), 2 (DR2) or 5 (DR5) nucleotides (Rochel and Moras, 2014). Others previously noted two potential RAREs in the 400 bp proximal *Stra8* promoter, one designated RARE1 (DR2 type, supported by ChIP experiments, Giuili et al., 2002; Kumar et al., 2011; Raverdeau et al., 2012), and the other designated as RARE2 (inverted repeat, IR5 type, Giuili et al., 2002), and one or both of these were found to be necessary for activation of the promoter by RA in F9 EC cells (Wang and Tilly, 2010). An additional putative RARE (DR4 type) has been noted ∼800 bp upstream of the transcription start site (TSS) (Raverdeau et al., 2012).

Using MatInspector, we analysed 5 kb of genomic DNA sequence upstream of the mouse *Stra8* TSS (Fig. S1). In addition to RARE1, we found numerous putative RAREs, but our analysis did not predict the unnamed RARE (DR4) (Raverdeau et al., 2012), nor RARE2 (Giuili et al., 2002). We did identify a putative RARE (DR1 type) partially overlapping with the previously noted IR5 type RARE2 site. We also identified a putative DMRT1-binding site that lies within the DMRT1-binding region previously identified by ChIP (Krentz et al., 2011), as well as others further upstream.

The 2.9 kb genomic region immediately upstream of the *Stra8* TSS is capable of recapitulating *in vivo Stra8* expression in fetal ovarian germ cells

When others made transgenic mouse lines, using random genomic integration, they were unable to detect transgene activation in fetal female germ cells using either 0.4 kb (Giuili et al., 2002) or 1.4 kb *Stra8* genomic fragments (Antonangeli et al., 2009; Nayernia et al., 2004; Sadate-Ngatchou et al., 2008), despite strong induction in the adult male testis. To determine whether the lack of induction in germ cells of the fetal ovary could be due to genomic integration effects, or insufficient regulatory sequence, we generated three lines of mice, each harbouring a single targeted copy of a transgene comprising *eGFP* driven by ∼1.4, ∼1.5 or ∼2.9 kb of *Stra8* putative promoter sequence (Fig. 1A). The 1.5 kb version was included because a previous study in F9 cells demonstrated that the 1.5 kb *Stra8* upstream genomic fragment has significant promoter activity (Kwon et al., 2014); the 2.9 kb *Stra8* promoter was the largest promoter length that we successfully inserted into the *Col1a1* locus. Because all three transgenes are inserted single-copy at the same defined open autosomal locus, 3′ to the *Col1a1* gene, expression levels in the three independent lines can be compared directly (Beard et al., 2006).

All three lines showed eGFP expression in the adult testes (Fig. S2) in a pattern similar to that of previously published transgene studies using the 0.4 kb and 1.4 kb *Stra8* promoter lengths (Giuili et al., 2002; Sadate-Ngatchou et al., 2008). Consistent with published reports, the 1.4 kb promoter fragments did not drive visible eGFP expression in the developing ovary, and this was also the case for the slightly larger 1.5 kb promoter fragment. However, the 2.9 kbStra8-eGFP transgene drove strong eGFP expression in fetal ovaries that could be visualized directly and proceeded in a dynamic anterior to posterior wave (Fig. 1B) similar to that well-established for endogenous *Stra8* expression (Bowles et al., 2006; Fu et al., 2017; Menke et al., 2003). Despite the fact that visible eGFP expression could not be detected for the

Development (2021) 148, dev194977. doi:10.1242/dev.194977

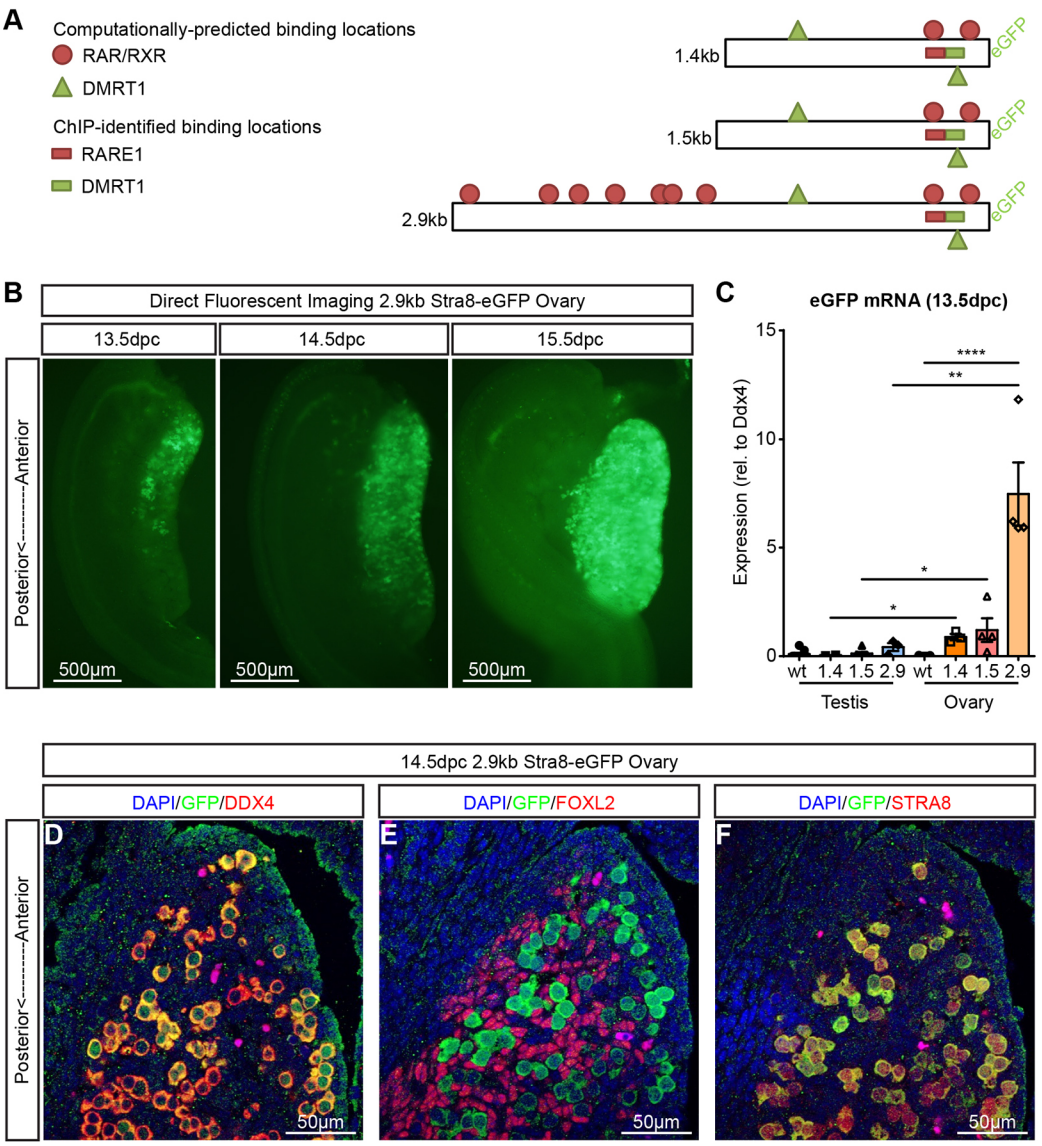

Fig. 1. The 2.9 kb *Stra8* promoter drives eGFP expression specifically in fetal ovarian germ cells. (A) Three different sized fragments of mouse *Stra8* promoter were used to drive eGFP expression in transgenic mice. Computationally predicted or ChIP-identified transcription factor binding sites for RAR/RXR and DMRT1 are noted. The + and – strand orientated putative binding sites are shown above and below the promoter fragments, respectively. (B) eGFP fluorescence driven by the 2.9 kb *Stra8* promoter is detectable by direct fluorescence imaging of fetal ovaries of transgenic mice, and shows the anterior to posterior wave that is characteristic of endogenous STRA8 expression. (C) Using qRT-PCR, the level of *eGFP* expression detected was higher in fetal ovarian tissue, compared with fetal testicular tissue, for all three lines. As expected, ovarian expression of eGFP was substantially higher when driven by the 2.9 kb *Stra8* promoter. Data are mean±s.e.m. **P*<0.05; ***P*<0.01; *****P*<0.0001; *n*=3-11 (unpaired two-tailed Student's *t*-test). (D) Immunofluorescence imaging of sections (anterior end of 14.5 dpc mouse ovary) demonstrated that eGFP signal is specific to germ cells (marked by DDX4). (E) eGFP does not overlap with FOXL2-expressing somatic cells. (F) There is a high degree of correlation between endogenous STRA8 signal and eGFP driven by the 2.9 kb *Stra8* promoter.

1.4 kb and 1.5 kb fragments, *eGFP* transcript detection was higher in fetal ovarian tissue than in testicular tissue at 13.5 dpc, as revealed by qRT-PCR analysis (Fig. 1C). Analysis of tissue sections of 2.9 kb ovaries by immunofluorescence showed eGFP staining only in germ cells (marked by DEAD box polypeptide 4, DDX4, Fig. 1D) and not in cells marked by the ovarian somatic cell marker forkhead box L2 (FOXL2; Fig. 1E). A close correlation was observed between the cytoplasmic eGFP and nuclear staining for endogenous STRA8 (Fig. 1F). When we quantified the co-expression of endogenous STRA8 and eGFP at 13.5 dpc, we found that eGFP was detectable in ∼68% of $STRA8^{+}$ germ cells, and there were no $eGFP^{+}/STRA8^{-}$ germ cells (Fig. S3A,B). Observations of 12.5 to 16.5 dpc 2.9 kbStra8-eGFP whole embryos under a fluorescence microscope, before and during dissection, did not reveal any significant eGFP signal outside of the developing ovary.

Together, these results demonstrate that the 2.9 kb genomic region immediately upstream of the *Stra8* TSS is sufficient to drive robust germ cell-specific eGFP expression in the mouse fetal ovary. Furthermore, we can conclude that regulatory elements included in this 2.9 kb fragment are sufficient to recapitulate the normal anterior to posterior 'wave' pattern of endogenous *Stra8* expression, with only a slight temporal lag in eGFP production compared with endogenous STRA8. Element(s) that respond in a sex-specific manner are present in the 1.4 kb and 1.5 kb fragments, as they drive higher levels of expression in the fetal ovary than fetal testis (Fig. 1C). In addition, our results indicate that element(s) crucial for

Development (2021) 148, dev194977. doi:10.1242/dev.194977

achieving high levels of expression in germ cells of the fetal ovary lie in the region between 1.5 kb and 2.9 kb upstream of the *Stra8* TSS.

Promoter activity can be modelled *in vitro* using the F9 EC cell line

Exploiting our finding that the 2.9 kb promoter fragment is capable of driving expression *in vivo*, we aimed to further characterise the functional elements of the *Stra8* promoter by *in vitro* analysis. To this end, we used the same promoter fragments (1.4, 1.5 and 2.9 kb) to drive firefly luciferase in the F9 EC cell line: we wanted to establish whether this line could be used to model ovarian germ cells with respect to *Stra8* expression. Transiently transfected F9 cells were cultured in medium containing either 50 nM RA or carrier (DMSO) for 18 h before assaying for luciferase activity. No significant differences were observed between the 1.4, 1.5 and 2.9 kb constructs treated with DMSO; however, in the presence of RA, all three promoters displayed substantially more luciferase activity than their respective controls (Fig. 2A, red hatched bars compared with dark grey bars).

We next investigated the possible regulation of *Stra8* by DMRT1 in this F9 model system. First, we tested whether RA induces endogenous *Dmrt1* expression in the F9 cell line: *Dmrt1* expression was basal in F9 cells and not substantially increased by RA

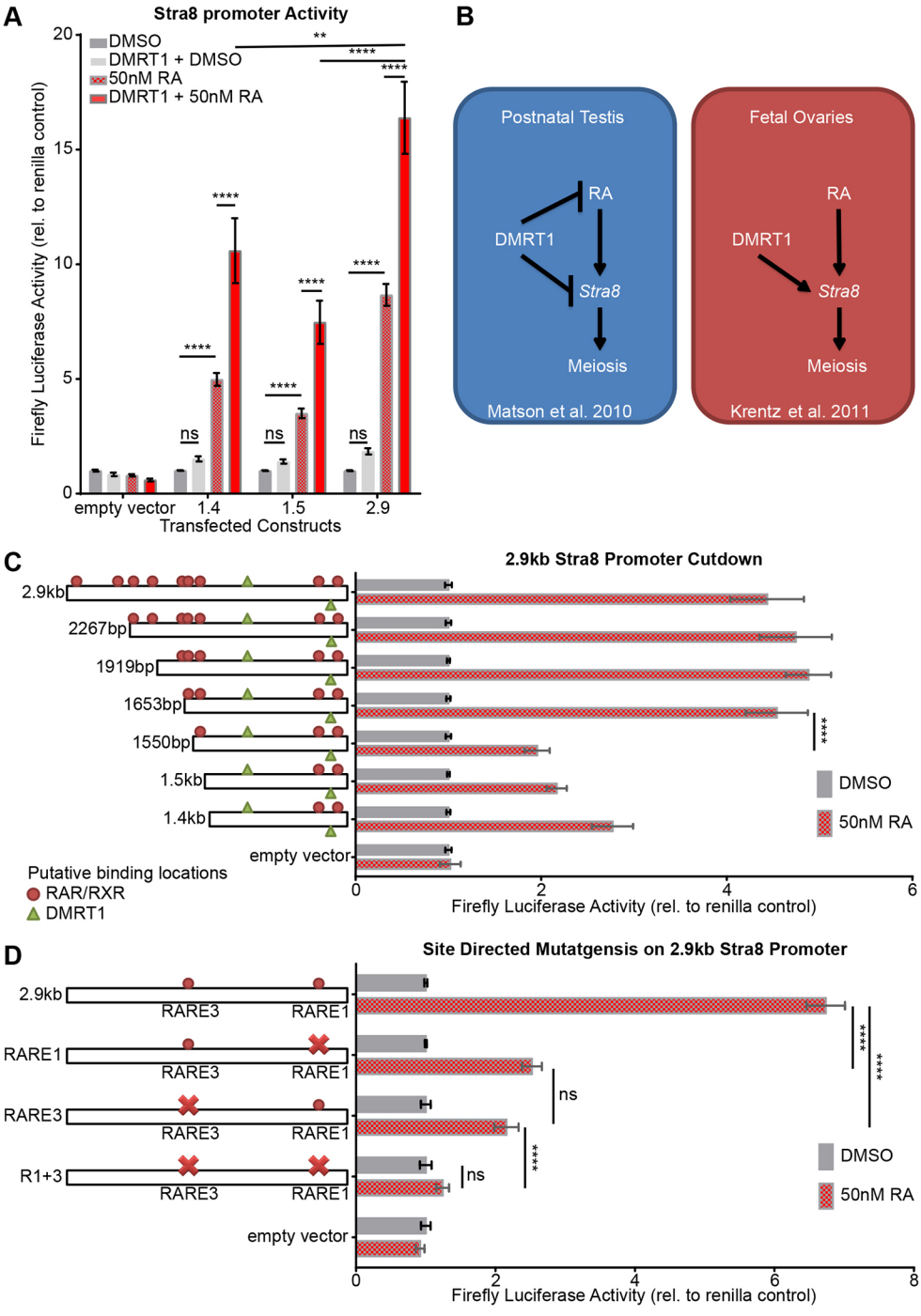

Fig. 2. F9 EC cells can be used to model the activity of the *Stra8* promoter in fetal ovarian germ cells. (A) Activity of the 2.9 kb, 1.5 kb and 1.4 kb promoters, when treated with RA, recapitulates trends observed in the *Stra8*-eGFP transgenic mice series, with the 2.9 kb promoter fragment driving the highest level of activity. Co-transfection with DMRT1 induced significant synergistic increases in the activity of all three *Stra8* promoter constructs. (B) The F9 EC cell line is useful to model *Stra8* expression in fetal ovarian germ cells as results are in accordance with published *in vivo* studies that concluded that DMRT1 promotes *Stra8* expression in the fetal ovary, whereas, in the postnatal testis, DMRT1 has a suppressive role. (C) *In vitro* assay of cutdown versions of the 2.9 kb *Stra8* promoter reveals a dramatic loss of activity when the promoter length is decreased from 1653 bp to 1550 bp. The deleted region includes a computationally predicted RARE we designate as RARE3. (D) Mutation of RARE3 significantly decreases the luciferase activity of the 2.9 kb promoter. A similar decrease is observed when RARE1 is mutated. When both RARE1 and RARE3 are mutated promoter activity is completely abolished in this *in vitro* system. Data are mean±s.e.m. Statistical significance was determined using unpaired two-tailed Student's *t*-test (C) or one-way (between constructs in A) or two-way ANOVA (D, and within construct in A). ***P*<0.01; *****P*<0.0001; ns=not significant (*n*=3).

Development (2021) 148, dev194977. doi:10.1242/dev.194977

treatment, and levels of *Dmrt1* expression were less than 10% of that detected in mouse fetal ovary tissue at 12.5 dpc (Fig. S4; Laursen et al., 2012). For all three *Stra8* promoter constructs, co-transfection with a *Dmrt1* expression construct alone did not significantly increase luciferase activity (Fig. 2A, light grey bars). However, in the presence of both RA and the *Dmrt1* expression construct, we observed an augmentation of luciferase activity and, as our *in vivo* studies would predict, the 2.9 kb fragment directed significantly more luciferase activity than its 1.4 kb and 1.5 kb counterparts (Fig. 2A, solid red bars). This apparent synergistic effect of DMRT1 and RA on the *Stra8* promoter constructs is consistent with evidence that DMRT1 can enhance *Stra8* expression in the fetal ovary (Krentz et al., 2011). As DMRT1 has a repressive effect on *Stra8* in the postnatal testis (Matson et al., 2010), the fetal ovarian-like response of our *Stra8* promoters in the presence of DMRT1 indicates that our approach of testing *Stra8* promoter constructs in F9 EC cells is suitable for modelling the regulation of *Stra8* in fetal ovarian germ cells (summarised in Fig. 2B).

Promoter deletion and site-directed mutagenesis studies demonstrate that RARE1 and RARE3 contribute to *Stra8* promoter activity *in vitro*

We systematically decreased the length of the 2.9 kb *Stra8* promoter construct to define the possible regulatory regions contributing to its greater sensitivity to RA, and continued to use F9 EC cells as an *in vitro* model system. No significant reduction in promoter activity was observed until the length was reduced from 1653 to 1550 bp (Fig. 2C). Within the intervening 103 bp region we identified a single putative RARE that we designated RARE3 (as RARE1 and RARE2 had previously been assigned for this promoter, Giuili et al., 2002).

To confirm RARE3 functionality in our *in vitro* F9 system, we mutated the site in the context of the full 2.9 kb *Stra8* luciferase construct and observed more than a 50% reduction in promoter activity (Fig. 2D). In a parallel experiment we also mutated RARE1, an element reported to bind RA receptors in ChIP experiments (Kumar et al., 2011; Raverdeau et al., 2012), and found a similar reduction in promoter activity. When both RAREs were simultaneously mutated the promoter no longer responded to RA in this system (Fig. 2D). These results show that both RARE1 and RARE3 are involved in regulating *Stra8* expression and, at least in our *in vitro* system, subtle mutation of both completely abolishes promoter activity. It also suggests that no other putative RAREs identified within the 2.9 kb region can direct expression in this system.

DMRT1/RA synergism is associated with the *Stra8* proximal promoter region

We next sought to address whether the synergistic effect of DMRT1 and RA (depicted in Fig. 2A) is specific to RARE1 (which is proximal to a ChIP-verified DMRT1 binding site; Fig. 1A; Murphy et al., 2010) or the more distal RARE3. We compared the unaltered and the RARE-mutated 2.9 kb *Stra8* promoter luciferase constructs in the presence or absence of the *Dmrt1* expression construct (Fig. 3A). We found that DMRT1 was still able to enhance the effects of RA on luciferase activity when RARE3 was mutated, but not when RARE1 was mutated (Fig. 3A, red hatched compared with solid red bars for RARE1 and RARE3 constructs). These results suggest that the synergism between DMRT1 and RA signalling is specific to the RARE1 site in this system.

We also mutated the DMRT1 binding site to test whether its loss has any effect on the ability of RA to promote transcription at the RARE1 site. DMRT1 was unable to promote transcription when either the RARE1 or the DMRT1 site were mutated (Fig. 3B). The ability of RA to elicit expression was retained when the DMRT1 site was mutated, and the level of activation was similar to that seen when RARE1 was mutated. This may mean that destruction of the DMRT1 site prevents signalling through the nearby RARE1 and that the observed RA response is due only to signalling through the intact RARE3. The lack of complete ablation of promoter activity when the DMRT1 site is mutated is consistent with reports showing that DMRT1-null females retain substantial *Stra8* expression and are fertile (Krentz et al., 2011). Overall, these results support the concept that RA plays a dominant instructive role and DMRT1 plays a supportive or enhancing role in regulating *Stra8* expression in the F9 cell culture model, acting together with RA at the RARE1 site (Fig. 3C).

Mutations in RARE1 and/or RARE3 mutation decrease expression of *Stra8 in vivo*

Results from our *in vitro* F9 cell studies suggest that RA acts directly to activate the 2.9 kb *Stra8* promoter, utilising both RARE1 and RARE3 sites, and that enhanced activity conferred by DMRT1 relies on an intact RARE1. To test whether these findings hold *in vivo*, we designed CRISPR/Cas9 reagents to specifically and subtly mutate the RAREs in the genomic *Stra8* promoter (Fig. S5A,B). Three mouse lines were established in which RARE1, RARE3 or both RAREs (RARE1/3) were mutated to reproduce the sequence changes employed in our *in vitro* constructs.

qRT-PCR analysis of 14.5 dpc ovaries from embryos with homozygous mutations of RARE1 revealed a significantly compromised *Stra8* transcription when compared with wild-type littermates (Fig. 4A; Fig. S6). This result correlates well with our observations regarding the importance of RARE1 for *Stra8* expression *in vitro*. Expression of *Rec8*, a meiotic marker induced by RA independently of STRA8 (Koubova et al., 2014), was not significantly altered, as expected. The diminished *Stra8* expression did not affect expression of meiotic markers *Sycp3* and *Dmc1* but *Pou5f1*, encoding the pluripotency marker POU5F1, was expressed at elevated levels, suggesting that differentiation of germ cells was compromised.

We examined *Stra8* expression in 14.5 dpc ovaries of the RARE3 mutant line and found that homozygous RARE3 mutants also had diminished levels of *Stra8* expression (Fig. 4B; Fig. S6), but the magnitude of the change was less than we observed for the RARE1 mutant, and less than predicted by our *in vitro* studies (Fig. 2D). As was the case for the RARE1 mutants, no significant changes were observed in *Rec8*, *Sycp3* and *Dmc1* expression, but *Pou5f1* expression was elevated.

We next analysed mice with mutations in both RARE1 and RARE3. Ovaries of 14.5 dpc embryos with the double mutation showed a more pronounced loss of *Stra8* expression (Fig. 4C; Fig. S6) but, unlike the case *in vitro*, we did not see a complete loss of *Stra8* expression. The retention of ∼45% of *Stra8* expression may indicate that active positive regulatory elements lie beyond the 2.9 kb promoter fragment that we used in our *in vitro* studies, and that these contribute to drive some *Stra8* expression *in vivo*. Whole-mount immunofluorescence showed that the residual STRA8 expression was predominantly at the anterior end of the gonad at 13.5 dpc, suggesting that the anterior to posterior wave is retained (Fig. S7). This result suggests that any remaining positive regulatory elements respond to signal(s) that originate at the anterior end of the gonad, or adjacent mesonephros, *in vivo*. It is possible that modification of RARE1 and RARE3 makes the locus less sensitive to RA and

Development (2021) 148, dev194977. doi:10.1242/dev.194977

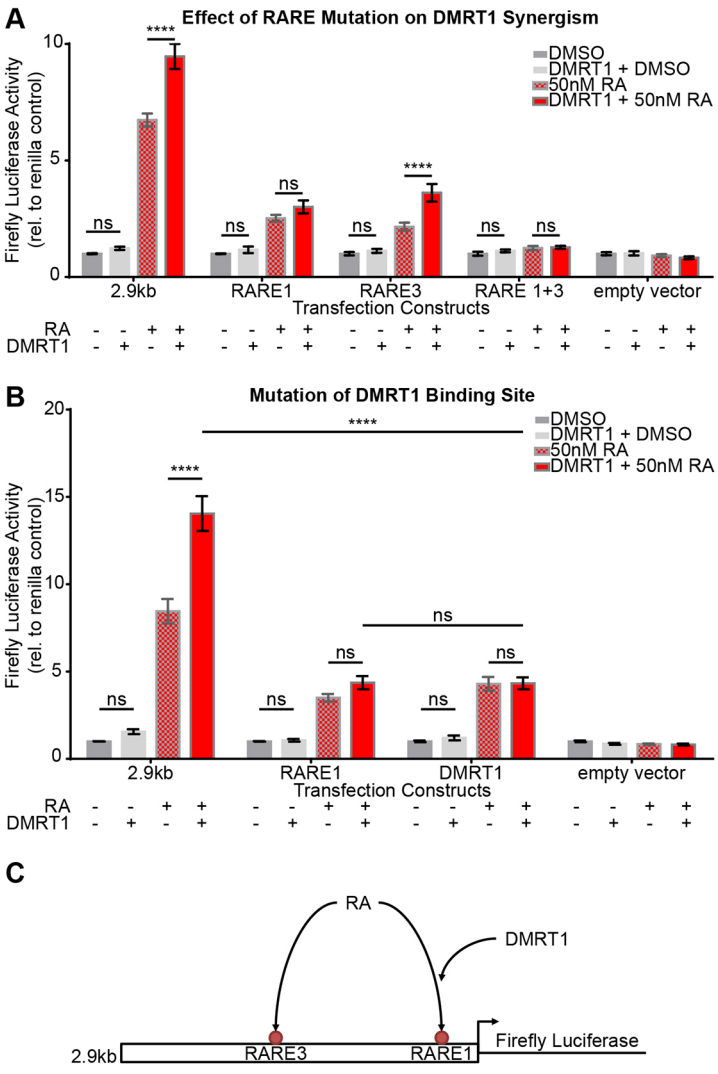

Fig. 3. The inducing effect of DMRT1 with respect to *Stra8* expression depends on the presence of an intact RARE1 *in vitro*. (A) The effect of DMRT1 on *Stra8* promoter activity is attenuated in F9 EC cells when RARE1 is mutated but not when RARE3 is mutated, suggesting site-specific synergistic interactions between DMRT1 and RAR/RXR proximal to the TSS. (B) Mutation of the DMRT1 binding site decreases but does not ablate promoter activity. (C) These results lead to a model in which RA signalling stimulates promoter activity at both RARE1 and RARE3, whereas DMRT1 interacts synergistically with RA signalling at RARE1 to enhance *Stra8* transcription. Data are mean±s.e.m. ****P<0.0001; ns=not significant (three-way ANOVA, n=3).

diminished *Stra8*/STRA8 expression in the double RARE mutant therefore reflects delayed onset of *Stra8* expression. We found that homozygous female mice harbouring RARE1, RARE3 or RARE1/3 double mutations were fertile. This is not unexpected given the largely unperturbed *Sycp3* and *Dmc1* expression observed at 14.5 dpc.

Deletion of 173 bp in the proximal promoter ablates *Stra8* expression

The CRISPR/Cas9 genome editing experiments leveraged the homology directed repair (HDR) pathway to introduce precise edits to our RARE sites of interest. In the absence of successful HDR, the non-homologous end joining (NHEJ) pathways assumes the DNA repair role; however, erroneous deletions of one to several hundred bases of DNA are often introduced to the target genomic region. During the generation of our RARE1 mutant, we also serendipitously generated a mouse line with a 173 bp deletion due to NHEJ (Δ173, −228 to −55 relative to the TSS; Fig. S5C). Intriguingly, the deleted region includes both RARE1 and the DMRT1 binding site (Fig. 5A). qRT-PCR analysis at 14.5 dpc showed that fetal ovaries homozygous for this mutation did not express *Stra8* at all, that expression of both *Dmc1* and *Sycp3* was substantially diminished, *Rec8* was unchanged and *Pou5f1* elevated (Fig. 5B). This result was corroborated by the lack of STRA8 and SYCP3 immunofluorescence staining in ovaries of the Δ173 mutant at 14.5 dpc compared with those of the wild type and RARE1/3 double mutant (Fig. 5C), and the retention of POU5F1$^+$ germ cells along the entire length of Δ173 mutant ovaries (Fig. S8). Breeding of homozygous Δ173 (n=4 each sex) animals with wild-type breeding partners for ∼3 months established that both sexes are infertile, whereas heterozygous breeders show no apparent abnormalities (Table S4). We replicated this 173 bp deletion in the context of the 2.9 kb *Stra8* promoter luciferase construct and saw no significant induction of promoter activity regardless of the presence of RA, DMRT1 or both (Fig. 5D). This result highlights the crucial importance of this small region of upstream sequence and confirms the relevance of our *in vitro* F9 EC cell model for examining early meiotic germline events.

DISCUSSION

STRA8 expression in germ cells is a necessary prelude to meiosis in both sexes, but it is not clear how the highly cell- and stage-specific control of *Stra8* expression is achieved. One major question relates to how the gene is so comprehensively silenced in somatic cells at all stages of development and adult life, and there is a growing appreciation of the various epigenetic mechanisms that appear to be involved in this silencing (Hargan-Calvopina et al., 2016; Wang and Tilly, 2008; Yokobayashi et al., 2013). In this study, however, we focused on the question of how *Stra8* expression is specifically

Development (2021) 148, dev194977. doi:10.1242/dev.194977

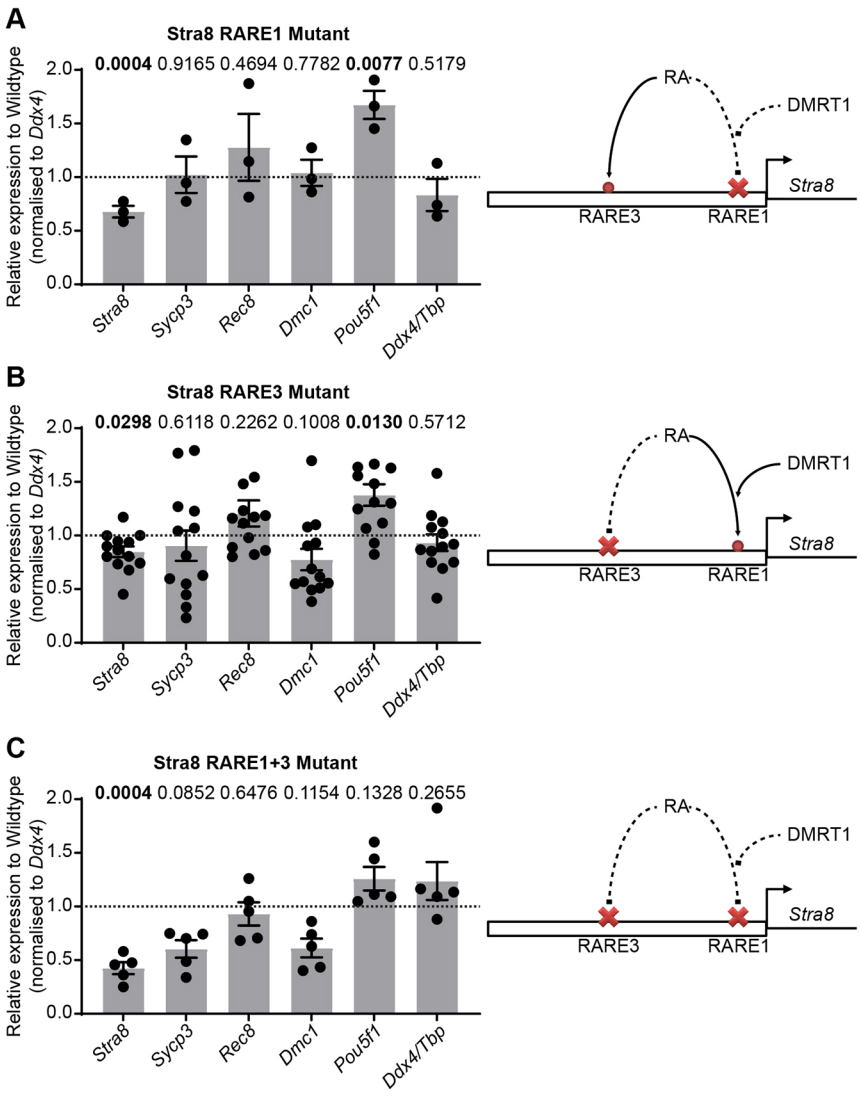

Fig. 4. Mice mutant for RARE1 or RARE3 have decreased *Stra8* expression and a corresponding retention of *Pou5f1* expression. (A) *Stra8* expression is decreased in the RARE1 homozygous mutant, whereas expression of *Rec8*, which is also regulated by RA, and expression of meiotic gene *Dmc1*, remains unchanged. Expression of pluripotency marker *Pou5f1* is retained in homozygous mutants. (B) Similar results, decreased *Stra8* and retention of *Pou5f1* expression, were observed in the RARE3 homozygous mutants, although the magnitude of changes in *Stra8* and *Pou5f1* expression were smaller. (C) *Stra8* expression is ∼45% of normal levels in the RARE1 and RARE3 double mutants. Data are mean±s.e.m. *P*-values are indicated above each column with significant difference in bold (unpaired two-tailed Student's *t*-test). Data point for each biological replicate is indicated by a solid circle.

activated in germ cells of the mouse fetal ovary, and in resolving the contentious question of whether RA plays a role in this crucial developmental step.

Previously, transgenic studies employing either 0.4 kb or 1.4 kb of *Stra8* upstream sequence reported high levels of germ cell-specific expression in the adult testis, but no expression was detected in the fetal ovary (Antonangeli et al., 2009; Giuili et al., 2002; Nayernia et al., 2004; Sadate-Ngatchou et al., 2008). Here, we generated a transgenic mouse line in which the 2.9 kb fragment immediately upstream of the mouse *Stra8* TSS was able to direct eGFP expression in a spatial and temporal pattern that recapitulates the expression of endogenous *Stra8* in germ cells of the mouse fetal ovary, with no eGFP induction observed in the fetal testis. We detected what appears to be a slight delay in the production of eGFP compared with endogenous STRA8: for $STRA8^{+}$ germ cells only 68% were also GFP^{+}, whereas no GFP^{+} germ cells were $STRA8^{-}$. This apparent lag might result from differences in transcriptional accessibility at the two distinct genomic loci (downstream of *Col1a1* and endogenous *Stra8*, respectively), in the timing required for RNA processing for the two transcripts, or in translation of the two proteins. It is also possible that the 2.9 kb promoter fragment lacks RAREs that impact on sensitivity to RA, or lacks binding sites for some other RA-independent inducing factor, compared with the endogenous *Stra8* locus. This line will be a valuable tool for dissecting the pre- and early-meiotic events that occur in female germ cells.

Targeting a single transgene copy into an open genomic locus, downstream of *Col1a1*, allowed us to directly compare the regulatory capability of the 2.9 kb fragment with that of the shorter 1.4 kb and 1.5 kb fragments. Although eGFP was not induced to a visible level with the shorter constructs, as previous studies had also found (Giuili et al., 2002; Sadate-Ngatchou et al., 2008), our *in vivo* studies revealed that the shorter transgenes were in fact transcriptionally activated in the fetal ovary (but not the fetal testis) and must, therefore, include some elements that respond in a sex-specific manner. We also found that, *in vivo*, regulatory element(s) that are important for high levels of expression must lie in the region between 2.9 kb and 1.5 kb upstream of the *Stra8* TSS.

We characterised the promoter elements required for expression of the transgene, working initially in F9 EC cells as a model for fetal germ cells. F9 cells are known to upregulate *Stra8* in response to RA and express modest levels of RARγ but low levels of RARα and RARβ (Laursen et al., 2012), which is a similar RAR profile to pre-meiotic ovarian germ cells at 10.5 dpc and 11.5 dpc (Vernet et al., 2020). Using a low dose of RA (50 nM), we identified a short distal regulatory region of ∼100 bp that was crucial for strong transcriptional

Development (2021) 148, dev194977. doi:10.1242/dev.194977

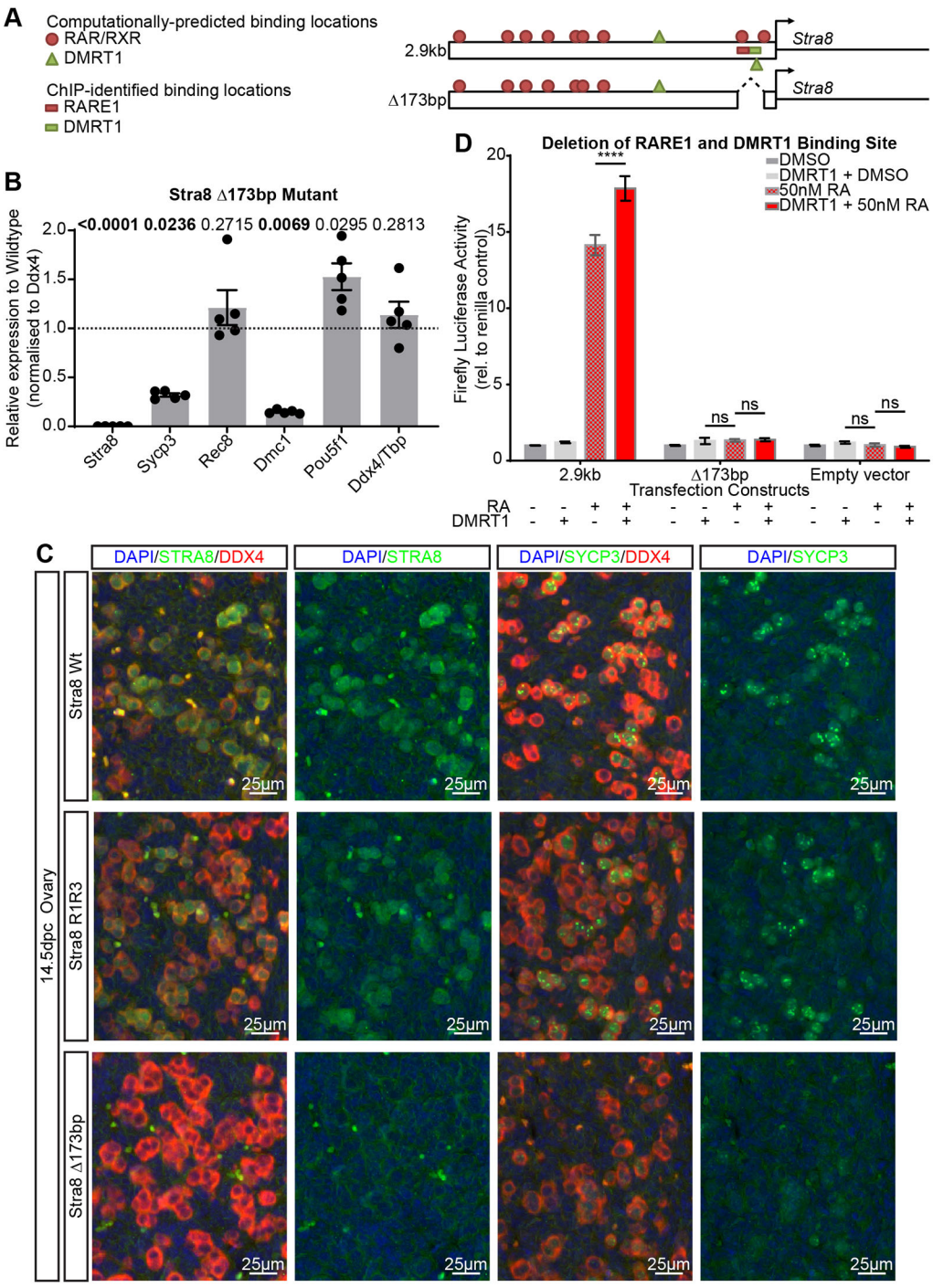

Fig. 5. Meiosis does not initiate and proceed in the fetal ovary of the Δ173 bp mouse. (A) The *Stra8* promoter region encompassing both RARE1 and DMRT1 binding sites is lost in the Δ173 bp mutant mice. (B) At 14.5 dpc, *Stra8* mRNA was undetectable in fetal ovaries of the Δ173 bp mouse. *Rec8* expression was unchanged but *Dmc1* and *Sycp3* expression was diminished, whereas *Pou5f1* expression was retained. (C) Loss of STRA8 protein was confirmed by immunofluorescence (XX ovary at 14.5 dpc). In addition, SYCP3 visualisation demonstrated that meiosis was not proceeding in the deletion mutant ovary. (D) Deletion of the 173 bp *Stra8* promoter region completely ablated luciferase activity in the *in vitro* culture system. Data are mean±s.e.m. Statistical significance was determined using unpaired two-tailed Student's *t*-test (B) or three-way ANOVA (D) (n=3). ****P<0.0001; ns=not significant (in B, P-values are indicated above each column with significant difference in bold). Data point for each biological replicate is indicated by a solid circle.

activation by RA. By way of site-directed mutagenesis, we demonstrated that a RARE sequence of the DR1 type, designated here as 'RARE3', lies within the region and is functional in our *in vitro* system. We also confirmed that RARE1 is active *in vitro*, as has been reported previously (Giuili et al., 2002). In light of these results, it seems likely that the additional upstream sequence between 1.5 kb and 2.9 kb, which includes RARE3, allows for greater sensitivity to the limited amount of RA available in the fetal ovary. The fact that shorter *Stra8* constructs direct detectable eGFP in the postnatal testis, but not the fetal ovary, is in line with evidence that higher levels of RA are present in the former than in the latter tissue (Bowles et al., 2016, 2006; Snyder et al., 2010).

There is substantial evidence that DMRT1 is an important regulator of *Stra8* but, paradoxically, it seems to enhance *Stra8* expression in germ cells of the fetal ovary (Krentz et al., 2011) and repress *Stra8* expression in adult spermatogonia (Matson et al., 2010). The effect in the fetal ovary seems to be somewhat stochastic, because some germ cells in the *Dmrt1*-null expressed STRA8 and entered meiosis normally, whereas others failed to do so (Krentz et al., 2011). In our F9 EC *in vitro* system, we found that DMRT1 alone had no effect on luciferase expression, but that its presence substantially enhanced the activation level achieved by RA. We further found that the ability of DMRT1 to positively influence *Stra8* expression, *in vitro*, required the more proximal RARE1

Development (2021) 148, dev194977. doi:10.1242/dev.194977

sequence to be intact, but not the distal RARE3 sequence. Moreover, mutation of the DMRT1 site previously defined by ChIP and located just 38 bp downstream of RARE1 (Krentz et al., 2011) ablated the DMRT1/RA synergistic effect. Our findings suggest a model whereby DMRT1 acts together with RA/RAR/RXR at the RARE1, whereas RA/RAR/RXR action at RARE3 is independent of DMRT1 and ensures, at least, an amplification of transcription (Fig. 3C). This conclusion is consistent with the observation that DMRT1 is present in germ cells of the fetal testis but that it does not induce *Stra8* expression and does not bind upstream of *Stra8* in that context (Krentz et al., 2011), presumably because RA is not present. Intriguingly, DMRT1 appears to inhibit, rather than enhance, RA-directed *Stra8* expression in adult spermatogonia (Matson et al., 2010); the molecular basis for this difference remains to be determined. For this reason, our F9 EC *in vitro* model is probably not suitable for modelling meiotic onset in postnatal spermatogonia, but our results suggest the F9 cell line is suited for investigating meiotic onset in fetal oocytes.

We aimed to validate our findings *in vivo*, and used CRISPR/Cas9 methodology to directly and subtly mutate RARE1 and RARE3 elements. Mutation of RARE1 had a greater effect than mutation of RARE3: *Stra8* expression fell to ∼65% and ∼85% of normal levels, respectively. When both RAREs were modified, *Stra8* expression was reduced further to ∼45% of normal. This is strong evidence that intact RARE1 and RARE3 binding sites are required for optimal *Stra8* expression. Nonetheless, ovarian fetal germ cells in the RARE1/3 mutant still entered meiosis and the homozygous XX adults were fertile; this is not surprising, as we found that downstream meiotic factors *Sycp3* and *Dmc1* remained relatively normal despite the reduced *Stra8* levels (Fig. 4C; Fig. S6). Interestingly, the residual expression of STRA8 in the RARE1/RARE3 double mutant ovaries is predominant at the anterior end of the gonad at 13.5 dpc, suggesting that any remaining intact positive regulatory elements respond to an anterior signal source; we consider it likely that this is RA, or some RA-induced factor, as levels are highest at the junction between the anterior gonad and mesonephros (Bowles et al., 2006). Although RARE2 (IR5) (Giuili et al., 2002), the RARE (DR4) found ∼800 bp upstream of the TSS, (Raverdeau et al., 2012) and the putative DR1-type RARE we identified proximal to the TSS, did not seem to function *in vitro*, it is possible that they do function *in vivo* if appropriate co-factors are present in that context. It is also possible that there are other important RA-sensitive regulatory elements, possibly including RAREs, beyond the 2.9 kb region or within the first intron of *Stra8*, that act to maintain *Stra8* expression in the absence of RARE1 and RARE3. One other possibility is that RA drives production of WNT4 predominantly at the anterior end of the gonad (Bowles et al., 2018), and that this is influencing *Stra8* expression in the germ cells (Chassot et al., 2011; Naillat et al., 2010).

Based on the recent findings of others, it is also possible that residual *Stra8* expression in fetal ovaries of the RARE1/3 mutant is due to BMP signalling (Miyauchi et al., 2017). However, unlike RA, there is no reason to anticipate that BMP is especially prevalent at the anterior end of the gonad, as *Bmp2* expression is observed in a rather homogeneous pattern along the length of the developing ovary (Yao et al., 2004). A downstream effector of BMP signalling, ZGLP1, has been shown, in mPGCLCs, to bind within the first intron of *Stra8*, but this occurs only in the presence of RA (Nagaoka et al., 2020). It is possible that, like DMRT1, ZGLP1 enhances *Stra8* expression only in the presence of RA (but not necessarily via RARE1 or RARE3). If this is the case, then it would make sense that that anterior to posterior wave would be retained in our RARE1/3 mutant, because RA levels are initially highest at the anterior end. The lack of *Zglp1* expression in F9 cells (Fig. S8; Laursen et al., 2012) suggests that the BMP signalling pathway is not active in our *in vitro* model; this may account for the discrepancy seen between our *in vitro* and *in vivo* results in terms of complete ablation or partially retained *Stra8* expression, respectively.

It is also possible that additional non-RA factor(s) are involved. A number of recent studies have supported the contention that induction of *Stra8* expression (and thus meiotic initiation) is independent of RA signalling in the fetal ovary, or at least that RA signalling is dispensable. It is reported that deletion of some or all of the known RA-synthesising enzymes diminishes *Stra8* expression but does not ablate it, and meiosis is still able to occur (Chassot et al., 2020; Kumar et al., 2011). Furthermore, deletion of RARs leads to delayed *Stra8* expression and fewer STRA8^{+} germ cells, but meiosis can still progress (Vernet et al., 2020). Our findings are not necessarily contradictory to these published works. We used an alternative and complementary strategy to investigate the role of RA in *Stra8* regulation and we provide direct evidence that, to achieve normal levels of *Stra8* expression in mouse fetal oocytes, it is necessary that two identified RAREs are intact: subtle mutation of both RARE1 and RARE3 diminishes *Stra8* expression by 55%, but does not deplete it entirely. Although residual *Stra8* expression may reflect RA acting at different RAREs or the actions of WNT(s) or BMP(s), as discussed above, it also remains possible that the remaining *Stra8* expression that we observed in this study is induced independently of RARs or RA-synthesising enzymes, as has been suggested (Chassot et al., 2020; Vernet et al., 2020), and that some additional as yet unidentified factor(s) are involved in ensuring *Stra8* expression in the context of the fetal ovarian germ cells.

We inadvertently made a 173 bp deletion of the *Stra8* proximal promoter that encompassed RARE1 and the DMRT1 binding site, but left the upstream RARE3 (identified here), RARE2 (Giuili et al., 2002) and a TATA box-like sequence (Giuili et al., 2002) intact (Fig. S5). We found that *Stra8* expression was ablated completely in fetal ovarian germ cells, that they did not enter meiosis, and that XX and XY individuals were infertile, suggesting that this line is effectively a *Stra8*-null. When this mutation was modelled *in vitro*, we similarly found a complete ablation of promoter activity. The severity of the effect, when compared with tandem *in vivo* mutation of RARE1 and RARE3, suggests that the deleted region includes at least some essential element of the 'core promoter' (though as noted, a TATA box-like sequence remains) and that its removal completely destroys the ability of transcription initiation complexes to bind and function. Future studies will focus on this short region of *Stra8* upstream sequence.

We conclude that *Stra8* is a direct target of RA in germ cells of the fetal ovary, and that sex-specific *Stra8* expression in this context is driven in part by canonical RA signalling, with RA/RAR complexes acting through RARE1 and newly identified RARE3. The inducing factor(s) that are responsible for the residual *Stra8* expression remain to be determined. We further conclude that the role of DMRT1 in driving *Stra8* expression is to enhance, when both RA and an intact RARE1 are present, rather than to instruct: this is in keeping with evidence that DMRT1 is more highly expressed in germ cells of the fetal testis than the fetal ovary and that *Dmrt1*-null females are fertile. Furthermore, we have demonstrated that 2.9 kb of *Stra8* upstream sequence is sufficient to recapitulate the curious anterior to posterior pattern of *Stra8* onset, and that the F9 EC cell culture system is suitable for modelling fetal germ cell meiotic onset. This information will underpin future studies of meiotic onset in the mouse model.

Development (2021) 148, dev194977. doi:10.1242/dev.194977

MATERIALS AND METHODS

Animal ethics

All procedures involving animals and their care conformed to institutional, state and national guidelines. This study was approved by the University of Queensland Animal Ethics Committee.

Mice

All transgenic mice were generated in house using stock C57BL/6J, CD1 and C57Bl/6JxCBA F1 hybrids purchased from Animal Resource Centre (Western Australia).

Stra8 promoter constructs

A fragment containing the 2.9 kb promoter region of *Stra8* was amplified from C57BL/6J genomic DNA using the 2.9 kbStra8_F and Stra8_R primers (Table S1). The PCR fragment was subcloned into pGEM-T-easy (Promega) and inserted into the XhoI/SacII site of pEGFP-N1 (Clontech) to generate the plasmid 2.9 kbStra8-eGFP. A similar plasmid, 1.4 kbStra8-eGFP, based on the work reported in Nayernia et al. (2004), was a kind gift from Julia Young and Kate Loveland (Monash University, Melbourne, Victoria, Australia). To assess the activity of the promoters *in vivo* the *Stra8* promoter, *eGFP* and polyA sequence from these constructs were cloned into the PGK/ATGfrt vector (MES4490, Thermo Scientific Open Biosystems) to allow targeted integration into ES cells (ESCs) and subsequent mouse line generation (further described in next section). Constructs for *in vitro* transfection assays used only the *Stra8* promoters from 2.9 kbStra8-eGFP and 1.4 kbStra8-eGFP, which were cloned into pGL4.10[luc2] (Promega) to generate *Stra8* promoter luciferase reporter constructs (see ensuing sections). The ATG start site of firefly luciferase precisely replaced the *eGFP* ATG start site of the constructs used for reporter mice generation.

Targeted integration of Stra8-eGFP constructs into ESCs and generation of transgenic reporter mice

The constructs 2.9 kbStra8-eGFP and 1.4 kbStra8-eGFP were excised with XhoI/SspI and SpeI/SspI, respectively. The 1.5 kbStra8-eGFP was prepared by digesting 2.9 kbStra8-eGFP with BspHI/SspI. All three Stra8-eGFP fragments were blunt-ended with Mung Bean Nuclease (New England Biolabs) before being ligated into the EcoRV site of the PGK/ATGfrt vector (MES4490, Thermo Scientific Open Biosystems). Orientation of the Stra8-eGFP inserts were determined by restriction enzyme digest and clones with the correct insert orientation for each promoter length were further validated by Sanger sequencing. The integration of Stra8-eGFP-PGK/ATGfrt constructs into KH2 ESCs (Beard et al., 2006) was carried out as described previously (Quinn et al., 2014). In brief, each Stra8-eGFP-PGK/ATGfrt construct was electroporated into KH2 ESCs along with FLPe recombinase-expressing construct (pCAGGS-FLPe-puro, MES4488, Thermo Scientific Open Biosystems). Positive colonies were selected using hygromycin before confirmation for correctly targeted integration (Col1a1-Geno7 and Col1a1-Geno8), as well as the presence of the Stra8-eGFP transgene (Stra8_Fw2 and eGFP_Rv1; Table S1). Correctly targeted cells were injected into C57BL/6J blastocysts and transferred into 0.5 dpc or 2.5 dpc pseudopregnant CD1 females. Chimeric founders were identified by coat colour and bred to C57BL/6J females to generate F1 progeny. Heterozygous pups identified by genotyping using the primers above were used to establish breeding colonies to supply mice for timed matings and subsequent analysis.

Timed matings and tissue collection

Stra8-eGFP and RARE mutant studs from each line were mated with females, with noon of the day that the copulatory plug was observed designated as 0.5 dpc. Embryos were collected from timed matings, between 12.5 dpc and 16.5 dpc. The sex of the embryos was either identified by visual inspection of dissected gonads or by genotyping of tail tissue for ubiquitin-like modifier activating enzyme 1 (*Uba1*, also known as *Ube1*) (Chuma and Nakatsuji, 2001). For qRT-PCR, individual gonads were dissected with the mesonephros removed, whereas for direct fluorescence imaging and whole-mount immunofluorescences the mesonephros was left on for orientation and referencing purposes. Whole embryos (minus tail for genotyping) were collected, fixed in 4% paraformaldehyde (PFA)/PBS and processed into paraffin for sectioning and immunofluorescence imaging.

qRT-PCR

Individual gonad pairs collected from each Stra8-eGFP line and RARE mutant lines were stored in RNAlater (76106, Qiagen) post-dissection. After genotyping, total RNA was extracted using an RNeasy Micro Kit (74106, Qiagen). Total RNA-containing eluate was immediately used for cDNA synthesis by reverse transcription using a High Capacity cDNA Reverse Transcription Kit (4368813, Life Technologies). All qRT-PCRs were performed on a Viia7 Real-Time PCR System (Life Technologies). *eGFP* transcripts were quantified using SYBR Green PCR master mix (Life Technologies) with primers GFP_F and GFP_R (Table S1). Relative expression levels were determined using the $2^{\text{delta-Ct}}$ method using germ cell-specific gene *Ddx4* (also known as *Mvh* and *Vasa*) with primers DDX4_F and DDX4_R (Table S1). For RARE1, RARE3, RARE1/3 and Δ173 mutant ovaries, expression levels of *Dmc1* (Mm00494485_m1), *Pou5f1* (Mm03053917_g1), *Rec8* (Mm00490939_m1), *Stra8* (Mm00486473_m1) and *Sycp3* (Mm00488519_m1) relative to *Ddx4* (Mm00802445t_m1) or *Tbp* (Mm01277045_m1) were quantified using Taqman Gene Expression Assays (Life Technologies). All kits and assays were performed according to instructions supplied by the manufacturer.

Direct fluorescence imaging

For direct fluorescence imaging of Stra8-eGFP gonads, freshly dissected gonads with mesonephros attached were placed in concave slides suspended in PBS with a glass coverslip. A BX-51 upright fluorescence microscope (Olympus) was used to visualise eGFP expression and images were captured using a DP70 colour camera (Olympus) attached to the microscope. Images were taken at multiple focal planes for each gonad and Adobe Photoshop CS5 version 12.0×64 was used for focus stacking using auto-stack, auto-align and auto-blend settings.

Section immunofluorescence imaging

Whole embryos embedded in paraffin were sectioned at 7 µm and immunofluorescence was performed as described previously (Bowles et al., 2010). Primary antibodies used were anti-DDX4 (1:1000, ab13840, rabbit polyclonal, Abcam), anti-FOXL2 (1:2000, rabbit polyclonal, Kashimada et al., 2011), anti-STRA8 (1:300, ab49405, rabbit polyclonal, Abcam), anti-GFP (1:100, ab5450, goat polyclonal), anti-SYCP3 (1:200, ab97672, Abcam) and anti-POU5F1 (1:200, sc-5279, Santa Cruz Biotechnology). Secondary antibodies used (at 1:200) were donkey anti–goat IgG Alexa Fluor 488 (A11055, Molecular Probes), donkey anti-rabbit IgG Alexa Fluor 568 (A10042, Molecular Probes) and donkey anti-mouse IgG Alexa Fluor 647 (A31571, Molecular Probes). Nuclei were stained with DAPI (20 µg/ml, D9542, Sigma Aldrich) and imaged with a Zeiss LSM710 attached to a Zeiss AxioExaminer Z1 Upright microscope.

Whole-mount immunofluorescence imaging and cell counting

Whole gonads and mesonephros were dissected out of the embryos and whole-mount immunofluorescence was performed as described previously with minor modifications (Hobbs et al., 2015). Briefly, dissected gonads were fixed in 4% PFA for 30 min at room temperature, washed in PBS before being blocked in PBS supplemented with 2% bovine serum albumin and 10% fetal bovine serum (FBS) for 4 h at 4°C. Gonads were then incubated overnight with primaries antibodies [anti-STRA8, 1:2000, ab49602 (Abcam); anti-GFP, 1:100, 338008 (Biolegend) and anti-TRA98, 1:500, ab82527 (Abcam)], followed by three washes of 30 min with PBS with 0.3% Triton X-100 before incubating for 4 h at 4°C with secondary antibodies [goat anti-rabbit IgG Alexa Fluor 594, A11037 (Invitrogen) and donkey anti-rat IgG Alexa Fluor 488, A21208 (Invitrogen)]. Nuclei were stained with DAPI (20 µg/ml, D9542, Sigma Aldrich) and imaged with a Leica DMi8 SP8 laser point scanning confocal microscope. $STRA8^{+}$ and GFP^{+} cells were manually counted using the cell counter plug-in of ImageJ. Briefly, cells were counted over a 30 µm *z*-stack at 4 *z*-planes (0, +10, +20 and +30 µm) for each biological replicate. At each plane, GFP^{+} and $STRA8^{+}$ were manually annotated in ImageJ and counts were generated by the cell counter plug-in.

Development (2021) 148, dev194977. doi:10.1242/dev.194977

F9 luciferase assays

F9 EC cells were obtained from the European Collection of Cell Cultures (ECACC, 85061803, Lot 00C011) via Cellbank Australia. Truncated transfection constructs were generated by restriction enzyme digest of the 2.9 kbStra8luc2 construct. Site-directed mutagenesis was used to mutate the putative transcription factor binding motifs RARE1 and RARE3 on the 2.9 kbStra8luc2 construct with the mutation design, including a SalI recognition site for identification purposes (mutations matched to those in RARE mutant mice, Table S2). Genotyping primers for RARE1 mutant mice were used to amplify the 173 bp deletion from mutant mice, which was used to replace the corresponding region on the 2.9 kbStra8luc2 construct for investigating promoter activity harbouring the 173 bp deletion *in vitro*. DMRT1 binding site mutation on the 2.9 kbStra8luc2 promoter was also performed using site-directed mutagenesis with the design including an AscI site for identification purposes. cDNA derived from F9 EC cells was used to amplify PCR products consisting of *Dmrt1* coding sequences that were subcloned into pGEM-T-easy (Promega) and then into pcDNA3.1 (Life Technologies) to create expression construct pDMRT1. F9 EC cells were cultured in 0.1% gelatin-coated flasks with high glucose Dulbecco's Modified Eagle Medium (DMEM, Gibco, 11995-073) supplemented with 10% v/v FBS (Bovogen, French Origin) and subcultured according to ECACC guidelines. For transfection experiments subconfluent (70-80%) F9 EC cells were treated with 0.25% trypsin (Gibco, 25200-072) before being seeded onto 24-well tissue culture plates at 2×10^5 cell/cm^2 and allowed to adhere overnight. Culture medium was replaced ∼1 h before transfection with Lipofectamine 2000 according to the manufacturer's instructions. Each well was transfected with 100 ng of one of the *Stra8* promoter-driven firefly luciferase constructs with or without 50 ng of pDMRT1. As a transfection control, 35 ng of *Renilla* luciferase construct pE1b-Rluc (a gift from Dr Liang Zhao (The University of Queensland, Brisbane, Queensland, Australia)) was also added to the transfection of each well, and pcDNA3.1 empty vector was used to make up for the DNA quantity required to maintain optimal DNA to lipfectamine ratios. Transfected cells were treated for 18 h the following day using medium supplemented with 1:2000 of either 100 µM all-trans-RA (R2625, Sigma Aldrich) or DMSO carrier control (final concentration of RA was 50 nM). Luciferase assays were then carried out using Dual-luciferase Reporter Assay System (Promega) and read with a POLARstar Omega plate reader (BMG Labtech) according to the manufacturer's instructions. The total culture duration of the F9 cell transfection experiments from seeding of the cells to harvesting for luciferase assay was controlled at 48 h.

Generation of *Stra8* promoter RARE mutant mice using CRISPR/Cas9 technology

Guide RNA was designed to target the sequence 5′-GGCGCTAGCCGCCTGGAT-3′ adjacent to RARE1. Oligonucleotides RARE1-top and RARE1-bottom were assembled and sgRNA was produced as described previously (Yang et al., 2013). For RARE3, custom DNA oligonucleotides RARE3_sgRNA_F, targeting the sequence 5′-CAAACCTCCACATTCCTCAC-3′, and a reusable chimeric_sgRNA_R (Table S1) were annealed and amplified using the Expand high fidelity PCR system (Roche). The PCR product consisted of a T7 promoter to drive transcription of sgRNA for RARE3 target sequence followed by chimeric guide RNA scaffold (Cong et al., 2013), and produces a 3′ DraI recognition site when T/A ligated. The PCR product was gel purified and T/A ligated into pGEM-T-easy (Promega) for Sanger sequencing using M13 primers. Correctly oriented clones with 100% sequence identity were digested with DraI, and the fragment containing the original PCR product, but not the T7 promoter from pGEM-T-easy, was gel purified for *in vitro* transcription (IVT). All sgRNAs were transcribed using a MEGAshortscript T7 Kit (Ambion), and Cas9 mRNA IVT was performed using an mMESSAGE mMACHINE T7 Transcription Kit (Ambion) from linearised pBS-Cas9 (gift from Dr Liang Zhao). IVT sgRNA and Cas9 mRNA were purified using a MEGAclear Transcription Clean-Up Kit (Ambion), with all procedures performed according to the manufacturer's instructions. Repair ssODN for RARE1 and RARE3 (RARE1_ssODN and RARE3_ssODN, respectively; Table S3) was designed with mutations to putative RAR/RXR binding sites, as well as an sgRNA protospacer adjacent motif recognition site to prevent retargeting and a SalI recognition site to facilitate genotype identification (identical mutations to F9 site-directed mutagenesis constructs). An injection cocktail consisting of 20 ng/µl Cas9 mRNA, 10 ng/µl sgRNA and 10 ng/µl ssODN was microinjected into the male pronucleus of one cell embryos derived from superovulated C56BL/6JxCBA F1 females. Injected embryos were cultured overnight in KSOM medium (Merck Millipore, MR-121-D) and embryos that reached the two-cell stage the next day were transferred into pseudopregnant CD1 females using standard methods. Mice harbouring correctly mutated RARE1 and/or RARE3 sites were identified by PCR using their respective genotyping primer pairs (Table S1) and then digested with SalI restriction enzyme. For the RARE1 and RARE3 double mutant, RARE1 mice were used to generate one-cell embryos for injection with RARE3 CRISPR/Cas9 injection cocktail. The Δ173 bp mutation was the result of NHEJ when generating the RARE1 mutant. The 2.9 kb *Stra8* promoter and first exon were PCR amplified, subcloned and sequenced from all mutant alleles (Fig. S9). No other mutations other than the intended RARE sites were introduced, but we did note the presence of known SNP rs40012028 in the RARE3 and Δ173 bp mutant alleles. We also amplified, cloned and sequenced exon 2 of the Δ173 bp mutant allele to confirm that there were no mutations in the ATG start codon and surrounding sequence (Fig. S9).

Computational predictions and statistics

Genomic DNA sequence (GRCm38.mm10) −5000 bp to +5000 bp relative to the *Stra8* TSS (start of RefSeq NM_009292.1) was used as input for transcription factor motif prediction in MatInspector (Cartharius et al., 2005; Quandt et al., 1995). GT-Scan (O'Brien and Bailey, 2014) and Optimized CRISPR Design (http://crispr.mit.edu) were used to identify putative CRISPR/Cas9 guide RNA targets. All statistical analysis was performed using GraphPad Prism 7 software.

Acknowledgements

We thank Dr Rudolf Jaenisch (Massachusetts Institute of Technology, Cambridge, MA, USA) and Dr Konrad Hochedlinger (Harvard University, Cambridge, MA, USA) for the gift of KH2 cells and Tara Davidson for technical assistance. We also acknowledge the School of Biomedical Sciences Core Facilities at the University of Queensland for use of the Leica DMi8 SP8 confocal microscope.

Competing interests

The authors declare no competing or financial interests.

Author contributions

Conceptualization: C.-W.F., P.K., J.B.; Methodology: C.-W.F., G.B., K.C., J.B.; Formal analysis: C.-W.F., G.B.; Investigation: C.-W.F.; Resources: K.C.; Data curation: C.-W.F., G.B., C.M.S., F.K.M.C., J.B.; Writing - original draft: C.-W.F., C.M.S., J.B.; Writing - review & editing: C.-W.F., C.M.S., P.K., J.B.; Supervision: C.M.S., P.K., J.B.; Project administration: P.K., J.B.; Funding acquisition: P.K., J.B.

Funding

This work was supported by the National Health and Medical Research Council, Australia (APP1109502 to J.B.) and the Australian Research Council (DP140104059 to J.B. and DP110105459 to P.K. and J.B.).

Supplementary information

Supplementary information available online at
https://dev.biologists.org/lookup/doi/10.1242/dev.194977.supplemental

Peer review history

The peer review history is available online at
https://dev.biologists.org/lookup/doi/10.1242/dev.194977.reviewer-comments.pdf

References

Anderson, E. L., Baltus, A. E., Roepers-Gajadien, H. L., Hassold, T. J., de Rooij, D. G., van Pelt, A. M. M. and Page, D. C. (2008). Stra8 and its inducer, retinoic acid, regulate meiotic initiation in both spermatogenesis and oogenesis in mice. *Proc. Natl. Acad. Sci. USA* **105**, 14976-14980. doi:10.1073/pnas.0807297105

Antonangeli, F., Giampietri, C., Petrungaro, S., Filippini, A. and Ziparo, E. (2009). Expression profile of a 400-bp Stra8 promoter region during spermatogenesis. *Microsc. Res. Tech.* **72**, 816-822. doi:10.1002/jemt.20724

Baltus, A. E., Menke, D. B., Hu, Y.-C., Goodheart, M. L., Carpenter, A. E., de Rooij, D. G. and Page, D. C. (2006). In germ cells of mouse embryonic ovaries,

the decision to enter meiosis precedes premeiotic DNA replication. *Nat. Genet.* **38**, 1430-1434. doi:10.1038/ng1919
Beard, C., Hochedlinger, K., Plath, K., Wutz, A. and Jaenisch, R. (2006). Efficient method to generate single-copy transgenic mice by site-specific integration in embryonic stem cells. *Genesis* **44**, 23-28. doi:10.1002/gene.20180
Bellutti, L., Abby, E., Tourpin, S., Messiaen, S., Moison, D., Trautmann, E., Guerquin, M.-J., Rouiller-Fabre, V., Habert, R. and Livera, G. (2019). Divergent Roles of CYP26B1 and endogenous retinoic acid in mouse fetal gonads. *Biomolecules* **9**, 536. doi:10.3390/biom9100536
Bowles, J., Knight, D., Smith, C., Wilhelm, D., Richman, J., Mamiya, S., Yashiro, K., Chawengsaksophak, K., Wilson, M. J., Rossant, J. et al. (2006). Retinoid signaling determines germ cell fate in mice. *Science* **312**, 596-600. doi:10.1126/science.1125691
Bowles, J., Feng, C.-W., Spiller, C., Davidson, T.-L., Jackson, A. and Koopman, P. (2010). FGF9 suppresses meiosis and promotes male germ cell fate in mice. *Dev. Cell* **19**, 440-449. doi:10.1016/j.devcel.2010.08.010
Bowles, J., Feng, C.-W., Miles, K., Ineson, J., Spiller, C. and Koopman, P. (2016). ALDH1A1 provides a source of meiosis-inducing retinoic acid in mouse fetal ovaries. *Nat. Commun.* **7**, 10845. doi:10.1038/ncomms10845
Bowles, J., Feng, C.-W., Ineson, J., Miles, K., Spiller, C. M., Harley, V. R., Sinclair, A. H. and Koopman, P. (2018). Retinoic acid antagonizes testis development in mice. *Cell Rep.* **24**, 1330-1341. doi:10.1016/j.celrep.2018.06.111
Cartharius, K., Frech, K., Grote, K., Klocke, B., Haltmeier, M., Klingenhoff, A., Frisch, M., Bayerlein, M. and Werner, T. (2005). MatInspector and beyond: promoter analysis based on transcription factor binding sites. *Bioinformatics* **21**, 2933-2942. doi:10.1093/bioinformatics/bti473
Chassot, A.-A., Gregoire, E. P., Lavery, R., Taketo, M. M., de Rooij, D. G., Adams, I. R. and Chaboissier, M.-C. (2011). RSPO1/β-catenin signaling pathway regulates oogonia differentiation and entry into meiosis in the mouse fetal ovary. *Plos ONE* **6**, e25641. doi:10.1371/journal.pone.0025641
Chassot, A.-A., Le Rolle, M., Jolivet, G., Stevant, I., Guigonis, J.-M., Da Silva, F., Nef, S., Pailhoux, E., Schedl, A., Ghyselinck, N. B. et al. (2020). Retinoic acid synthesis by ALDH1A proteins is dispensable for meiosis initiation in the mouse fetal ovary. *Sci. Adv.* **6**, eaaz1261. doi:10.1126/sciadv.aaz1261
Chuma, S. and Nakatsuji, N. (2001). Autonomous transition into meiosis of mouse fetal germ cells in vitro and its inhibition by gp130-mediated signaling. *Dev. Biol.* **229**, 468-479. doi:10.1006/dbio.2000.9989
Cong, L., Ran, F. A., Cox, D., Lin, S., Barretto, R., Habib, N., Hsu, P. D., Wu, X., Jiang, W., Marraffini, L. A. et al. (2013). Multiplex genome engineering using CRISPR/Cas systems. *Science* **339**, 819-823. doi:10.1126/science.1231143
Fu, X.-F., Yang, F., Cheng, S.-F., Feng, Y.-N., Li, L., Dyce, P. W., Shen, W. and Sun, X.-F. (2017). The epigenetic modifications and the anterior to posterior characterization of meiotic entry during mouse oogenesis. *Histochem. Cell Biol.* **148**, 61-72. doi:10.1007/s00418-017-1545-9
Giuili, G., Tomljenovic, A., Labrecque, N., Oulad-Abdelghani, M., Rassoulzadegan, M. and Cuzin, F. (2002). Murine spermatogonial stem cells: targeted transgene expression and purification in an active state. *EMBO Rep.* **3**, 753-759. doi:10.1093/embo-reports/kvf149
Griswold, M. D., Hogarth, C. A., Bowles, J. and Koopman, P. (2012). Initiating meiosis: the case for retinoic acid. *Biol. Reprod.* **86**, 35. doi:10.1095/biolreprod.111.096610
Hargan-Calvopina, J., Taylor, S., Cook, H., Hu, Z., Lee, S. A., Yen, M.-R., Chiang, Y.-S., Chen, P.-Y. and Clark, A. T. (2016). Stage-specific demethylation in primordial germ cells safeguards against precocious differentiation. *Dev. Cell* **39**, 75-86. doi:10.1016/j.devcel.2016.07.019
Hobbs, R. M., La, H. M., Mäkelä, J.-A., Kobayashi, T., Noda, T. and Pandolfi, P. P. (2015). Distinct germline progenitor subsets defined through Tsc2–mTORC1 signaling. *EMBO Rep.* **16**, 467-480. doi:10.15252/embr.201439379
Kashimada, K., Pelosi, E., Chen, H., Schlessinger, D., Wilhelm, D. and Koopman, P. (2011). FOXL2 and BMP2 act cooperatively to regulate follistatin gene expression during ovarian development. *Endocrinology* **152**, 272-280. doi:10.1210/en.2010-0636
Kojima, M. L., de Rooij, D. G. and Page, D. C. (2019). Amplification of a broad transcriptional program by a common factor triggers the meiotic cell cycle in mice. *eLife* **8**, e43738. doi:10.7554/eLife.43738
Koubova, J., Menke, D. B., Zhou, Q., Capel, B., Griswold, M. D. and Page, D. C. (2006). Retinoic acid regulates sex-specific timing of meiotic initiation in mice. *Proc. Natl. Acad. Sci. USA* **103**, 2474-2479. doi:10.1073/pnas.0510813103
Koubova, J., Hu, Y.-C., Bhattacharyya, T., Soh, Y. Q. S., Gill, M. E., Goodheart, M. L., Hogarth, C. A., Griswold, M. D. and Page, D. C. (2014). Retinoic acid activates two pathways required for meiosis in mice. *PLoS Genet.* **10**, e1004541. doi:10.1371/journal.pgen.1004541
Krentz, A. D., Murphy, M. W., Sarver, A. L., Griswold, M. D., Bardwell, V. J. and Zarkower, D. (2011). DMRT1 promotes oogenesis by transcriptional activation of Stra8 in the mammalian fetal ovary. *Dev. Biol.* **356**, 63-70. doi:10.1016/j.ydbio.2011.05.658
Kuang, S., Li, H., Feng, J., Xu, S. and Le, Y. (2019). Correlation of BRCA2 gene mutation and prognosis as well as variant genes in invasive urothelial carcinoma of the bladder. *Cancer Biomark.* **25**, 203-212. doi:10.3233/CBM-182379
Kumar, S., Chatzi, C., Brade, T., Cunningham, T. J., Zhao, X. and Duester, G. (2011). Sex-specific timing of meiotic initiation is regulated by Cyp26b1 independent of retinoic acid signalling. *Nat. Commun.* **2**, 151. doi:10.1038/ncomms1136
Kumar, S., Cunningham, T. J. and Duester, G. (2013). Resolving molecular events in the regulation of meiosis in male and female germ cells. *Sci. Signal.* **6**, pe25. doi:10.1126/scisignal.2004530
Kwon, J. T., Jin, S., Choi, H., Kim, J., Jeong, J., Kim, J., Kim, Y., Cho, B.-N. and Cho, C. (2014). Identification and characterization of germ cell genes expressed in the F9 testicular teratoma stem cell line. *PLoS ONE* **9**, e103837. doi:10.1371/journal.pone.0103837
Laursen, K. B., Wong, P. M. and Gudas, L. J. (2012). Epigenetic regulation by RARα maintains ligand-independent transcriptional activity. *Nucleic Acids Res.* **40**, 102-115. doi:10.1093/nar/gkr637
Li, H. and Clagett-Dame, M. (2009). Vitamin A deficiency blocks the initiation of meiosis of germ cells in the developing rat ovary in vivo. *Biol. Reprod.* **81**, 996-1001. doi:10.1095/biolreprod.109.078808
MacLean, G., Li, H., Metzger, D., Chambon, P. and Petkovich, M. (2007). Apoptotic extinction of germ cells in testes of Cyp26b1 knockout mice. *Endocrinology* **148**, 4560-4567. doi:10.1210/en.2007-0492
Mark, M., Ghyselinck, N. B. and Chambon, P. (2006). Function of retinoid nuclear receptors: lessons from genetic and pharmacological dissections of the retinoic acid signaling pathway during mouse embryogenesis. *Annu. Rev. Pharmacol. Toxicol.* **46**, 451-480. doi:10.1146/annurev.pharmtox.46.120604.141156
Mark, M., Jacobs, H., Oulad-Abdelghani, M., Dennefeld, C., Feret, B., Vernet, N., Codreanu, C.-A., Chambon, P. and Ghyselinck, N. B. (2008). STRA8-deficient spermatocytes initiate, but fail to complete, meiosis and undergo premature chromosome condensation. *J. Cell Sci.* **121**, 3233-3242. doi:10.1242/jcs.035071
Matson, C. K., Murphy, M. W., Griswold, M. D., Yoshida, S., Bardwell, V. J. and Zarkower, D. (2010). The mammalian doublesex homolog DMRT1 is a transcriptional gatekeeper that controls the mitosis versus meiosis decision in male germ cells. *Dev. Cell* **19**, 612-624. doi:10.1016/j.devcel.2010.09.010
Menke, D. B., Koubova, J. and Page, D. C. (2003). Sexual differentiation of germ cells in XX mouse gonads occurs in an anterior-to-posterior wave. *Dev. Biol.* **262**, 303-312. doi:10.1016/S0012-1606(03)00391-9
Miyauchi, H., Ohta, H., Nagaoka, S., Nakaki, F., Sasaki, K., Hayashi, K., Yabuta, Y., Nakamura, T., Yamamoto, T. and Saitou, M. (2017). Bone morphogenetic protein and retinoic acid synergistically specify female germ-cell fate in mice. *EMBO J.* **36**, 3100-3119. doi:10.15252/embj.201796875
Mu, X., Wen, J., Guo, M., Wang, J., Li, G., Wang, Z., Wang, Y., Teng, Z., Cui, Y. and Xia, G. (2013). Retinoic acid derived from the fetal ovary initiates meiosis in mouse germ cells. *J. Cell. Physiol.* **228**, 627-639. doi:10.1002/jcp.24172
Murphy, M. W., Sarver, A. L., Rice, D., Hatzi, K., Ye, K., Melnick, A., Heckert, L. L., Zarkower, D. and Bardwell, V. J. (2010). Genome-wide analysis of DNA binding and transcriptional regulation by the mammalian Doublesex homolog DMRT1 in the juvenile testis. *Proc. Natl. Acad. Sci. USA* **107**, 13360-13365. doi:10.1073/pnas.1006243107
Nagaoka, S. I., Nakaki, F., Miyauchi, H., Nosaka, Y., Ohta, H., Yabuta, Y., Kurimoto, K., Hayashi, K., Nakamura, T., Yamamoto, T. et al. (2020). ZGLP1 is a determinant for the oogenic fate in mice. *Science* **367**, eaaw4115. doi:10.1126/science.aaw4115
Naillat, F., Prunskaite-Hyyryläinen, R., Pietilä, I., Sormunen, R., Jokela, T., Shan, J. and Vainio, S. J. (2010). Wnt4/5a signalling coordinates cell adhesion and entry into meiosis during presumptive ovarian follicle development. *Hum. Mol. Genet.* **19**, 1539-1550. doi:10.1093/hmg/ddq027
Nayernia, K., Li, M., Jaroszynski, L., Khusainov, R., Wulf, G., Schwandt, I., Korabiowska, M., Michelmann, H. W., Meinhardt, A. and Engel, W. (2004). Stem cell based therapeutical approach of male infertility by teratocarcinoma derived germ cells. *Hum. Mol. Genet.* **13**, 1451-1460. doi:10.1093/hmg/ddh166
O'Brien, A. and Bailey, T. L. (2014). GT-Scan: identifying unique genomic targets. *Bioinformatics* **30**, 2673-2675. doi:10.1093/bioinformatics/btu354
Ohta, K., Lin, Y., Hogg, N., Yamamoto, M. and Yamazaki, Y. (2010). Direct effects of retinoic acid on entry of fetal male germ cells into meiosis in mice. *Biol. Reprod.* **83**, 1056-1063. doi:10.1095/biolreprod.110.085787
Oulad-Abdelghani, M., Bouillet, P., Décimo, D., Gansmuller, A., Heyberger, S., Dollé, P., Bronner, S., Lutz, Y. and Chambon, P. (1996). Characterization of a premeiotic germ cell-specific cytoplasmic protein encoded by Stra8, a novel retinoic acid-responsive gene. *J. Cell Biol.* **135**, 469-477. doi:10.1083/jcb.135.2.469
Quandt, K., Frech, K., Karas, H., Wingender, E. and Werner, T. (1995). MatInd and MatInspector: new fast and versatile tools for detection of consensus matches in nucleotide sequence data. *Nucleic Acids Res.* **23**, 4878-4884. doi:10.1093/nar/23.23.4878
Quinn, A., Kashimada, K., Davidson, T.-L., Ng, E. T., Chawengsaksophak, K., Bowles, J. and Koopman, P. (2014). A site-specific, single-copy transgenesis strategy to identify 5′ regulatory sequences of the mouse testis-determining gene Sry. *PLoS ONE* **9**, e94813. doi:10.1371/journal.pone.0094813
Raverdeau, M., Gely-Pernot, A., Feret, B., Dennefeld, C., Benoit, G., Davidson, I., Chambon, P., Mark, M. and Ghyselinck, N. B. (2012). Retinoic acid induces Sertoli cell paracrine signals for spermatogonia differentiation but cell

autonomously drives spermatocyte meiosis. *Proc. Natl. Acad. Sci. USA* **109**, 16582-16587. doi:10.1073/pnas.1214936109

Rochel, N. and Moras, D. (2014). Architecture of DNA Bound RAR Heterodimers. *Subcell. Biochem.* **70**, 21-36. doi:10.1007/978-94-017-9050-5_2

Rossant, J., Zirngibl, R., Cado, D., Shago, M. and Giguere, V. (1991). Expression of a retinoic acid response element-hsplacZ transgene defines specific domains of transcriptional activity during mouse embryogenesis. *Genes Dev.* **5**, 1333-1344. doi:10.1101/gad.5.8.1333

Sadate-Ngatchou, P. I., Payne, C. J., Dearth, A. T. and Braun, R. E. (2008). Cre recombinase activity specific to postnatal, premeiotic male germ cells in transgenic mice. *Genesis* **46**, 738-742. doi:10.1002/dvg.20437

Snyder, E. M., Small, C. and Griswold, M. D. (2010). Retinoic acid availability drives the asynchronous initiation of spermatogonial differentiation in the mouse. *Biol. Reprod.* **83**, 783-790. doi:10.1095/biolreprod.110.085811

Tedesco, M., Desimio, M. G., Klinger, F. G., De Felici, M. and Farini, D. (2013). Minimal concentrations of retinoic acid induce stimulation by retinoic acid 8 and promote entry into meiosis in isolated pregonadal and gonadal mouse primordial germ cells. *Biol. Reprod.* **88**, 145. doi:10.1095/biolreprod.112.106526

Trautmann, E., Guerquin, M.-J., Duquenne, C., Lahaye, J.-B., Habert, R. and Livera, G. (2008). Retinoic acid prevents germ cell mitotic arrest in mouse fetal testes. *Cell Cycle* **7**, 656-664. doi:10.4161/cc.7.5.5482

Vernet, N., Condrea, D., Mayere, C., Féret, B., Klopfenstein, M., Magnant, W., Alunni, V., Telentin, M., Souali-Crespo, S., Nef, S. et al. (2020). Meiosis occurs normally in the fetal ovary of mice lacking all retinoic acid receptors. *Sci. Adv.* **6**, eaaz1139. doi:10.1126/sciadv.aaz1139

Wang, N. and Tilly, J. (2008). Inhibition of histone deacetylase activity amplifies retinoic acid-mediated induction of Stra8 expression and oogenesis in ovaries of adult female mice. *Biol. Reprod.* **78**, 122-122. doi:10.1093/biolreprod/78.s1.122

Wang, N. and Tilly, J. L. (2010). Epigenetic status determines germ cell meiotic commitment in embryonic and postnatal mammalian gonads. *Cell Cycle* **9**, 339-349. doi:10.4161/cc.9.2.10447

Wang, S., Wang, X., Ma, L., Lin, X., Zhang, D., Li, Z., Wu, Y., Zheng, C., Feng, X., Liao, S. et al. (2016). Retinoic acid is sufficient for the in vitro induction of mouse spermatocytes. *Stem Cell Rep.* **7**, 80-94. doi:10.1016/j.stemcr.2016.05.013

Yang, H., Wang, H., Shivalila, C. S., Cheng, A. W., Shi, L. and Jaenisch, R. (2013). One-step generation of mice carrying reporter and conditional alleles by CRISPR/Cas-mediated genome engineering. *Cell* **154**, 1370-1379. doi:10.1016/j.cell.2013.08.022

Yao, H. H. C., Matzuk, M. M., Jorgez, C. J., Menke, D. B., Page, D. C., Swain, A. and Capel, B. (2004). Follistatin operates downstream of Wnt4 in mammalian ovary organogenesis. *Dev. Dyn.* **230**, 210-215. doi:10.1002/dvdy.20042

Yokobayashi, S., Liang, C.-Y., Kohler, H., Nestorov, P., Liu, Z., Vidal, M., van Lohuizen, M., Roloff, T. C. and Peters, A. H. F. M. (2013). PRC1 coordinates timing of sexual differentiation of female primordial germ cells. *Nature* **495**, 236-240. doi:10.1038/nature11918

Supplementary Information

Supplementary Figures
Figure S1

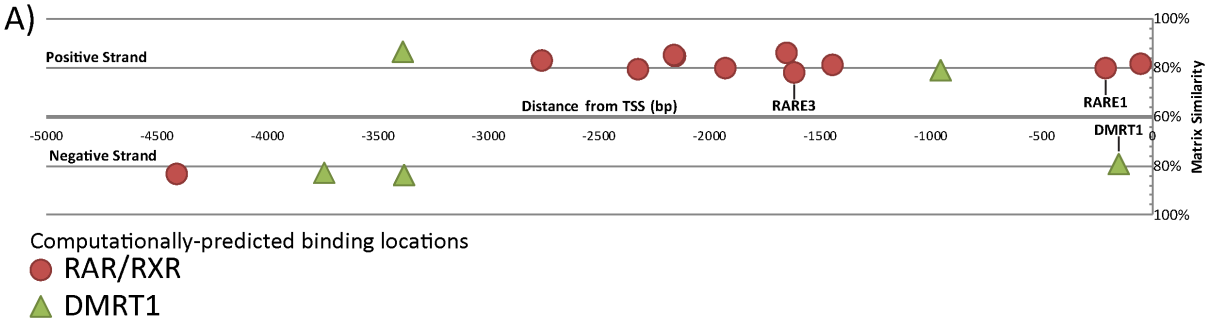

Transcription Factor Matrix	Start position	End position	Strand	Matrix sim.	Sequence
Retinoic acid receptor / retinoid X receptor heterodimer	-4418	-4394	-	0.833	AGGAGGATCGTTGCCAGTTCAAGAA
	-2774	-2750	+	0.831	ACTCCTCTGGCTCAGAGGTCTTTAG
	-2337	-2313	+	0.797	ACAAACCAGGACCAAAGGACATTGA
	-2176	-2152	+	0.856	CAGGGATGCGGTCATAGGCCACAGG
	-2169	-2145	+	0.852	GCGGTCATAGGCCACAGGGCATACG
	-1942	-1918	+	0.799	AAGTTCAAAGGATAGTGGTCATATG
	-1667	-1643	+	0.862	GCTGAGACCTGTCAGAGGTCAAAGT
	-1634	-1610	+	0.785	CTCCACATTCCTCACAGGTCAAGGA
	-1459	-1435	+	0.816	AGAGTCAGAAGGGATAGGTCATGAC
	-221	-197	+	0.803	CTGGATGGGGTGAAAAGGTCATCTT
	-65	-41	+	0.817	GCAGCCTGGGGTACCAGGTCAGTTT
Doublesex and mab-3 related transcription factor 1	-3754	-3734	-	0.828	GTGAGAAGGGACATTGTGGGA
	-3400	-3380	+	0.869	GTATGTTGGCACACTGTATCC
	-3394	-3374	-	0.833	GGCTGGGGATACAGTGTGCCA
	-968	-948	+	0.793	AATTTAAGGTACCCTGTTGCA
	-161	-141	-	0.789	ATTGGTGAAAACATTGTAACA

Figure S1: Computational prediction of RAR/RXR and DMRT1 binding sites 5kb upstream of *Stra8* TSS using MatInspector.

Graphical representation of the location of putative RAR/RXR (red circle) and DMRT1 (green triangle) binding sites in relation to TSS of *Stra8*. Identified binding sites on the positive strand and negative strands are shown above and below the midline respectively. Putative binding sites are called when matrix similarity is >0.75, and this is indicated by their distance away from the midline; sites further away have higher similarity scores. Binding sites corresponding to RARE1, RARE3 and DMRT1 examined in this study are also indicated.

Figure S2

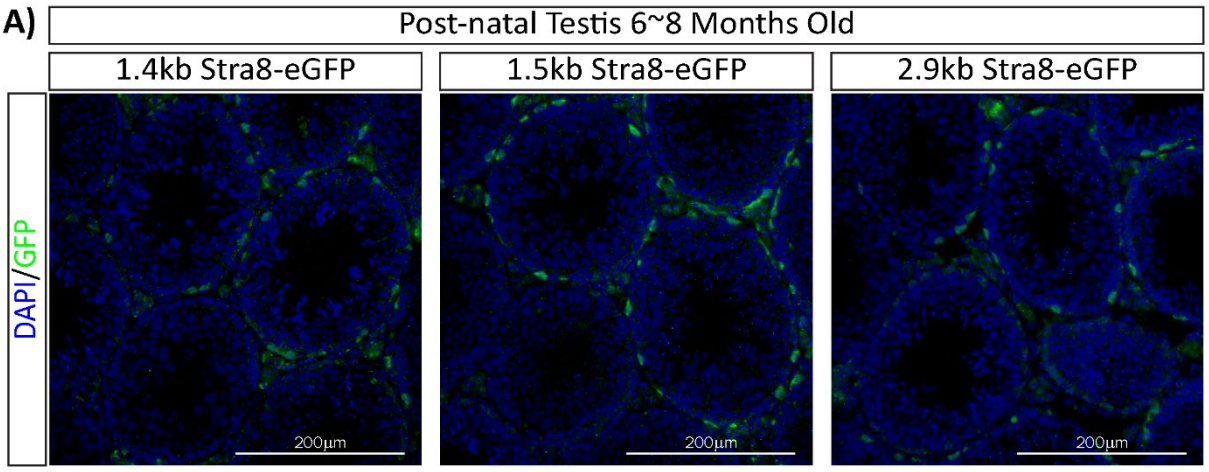

Figure S2: Testicular expression of eGFP is similar among in all three *Stra8* promoter lines. Immunofluorescent analysis of adult testis for eGFP expression shows that, in all three lines, GFP is detectable in a pattern similar to that observed in previous studies (Giuili et al., 2002; Sadate-Ngatchou et al., 2008).

Figure S3

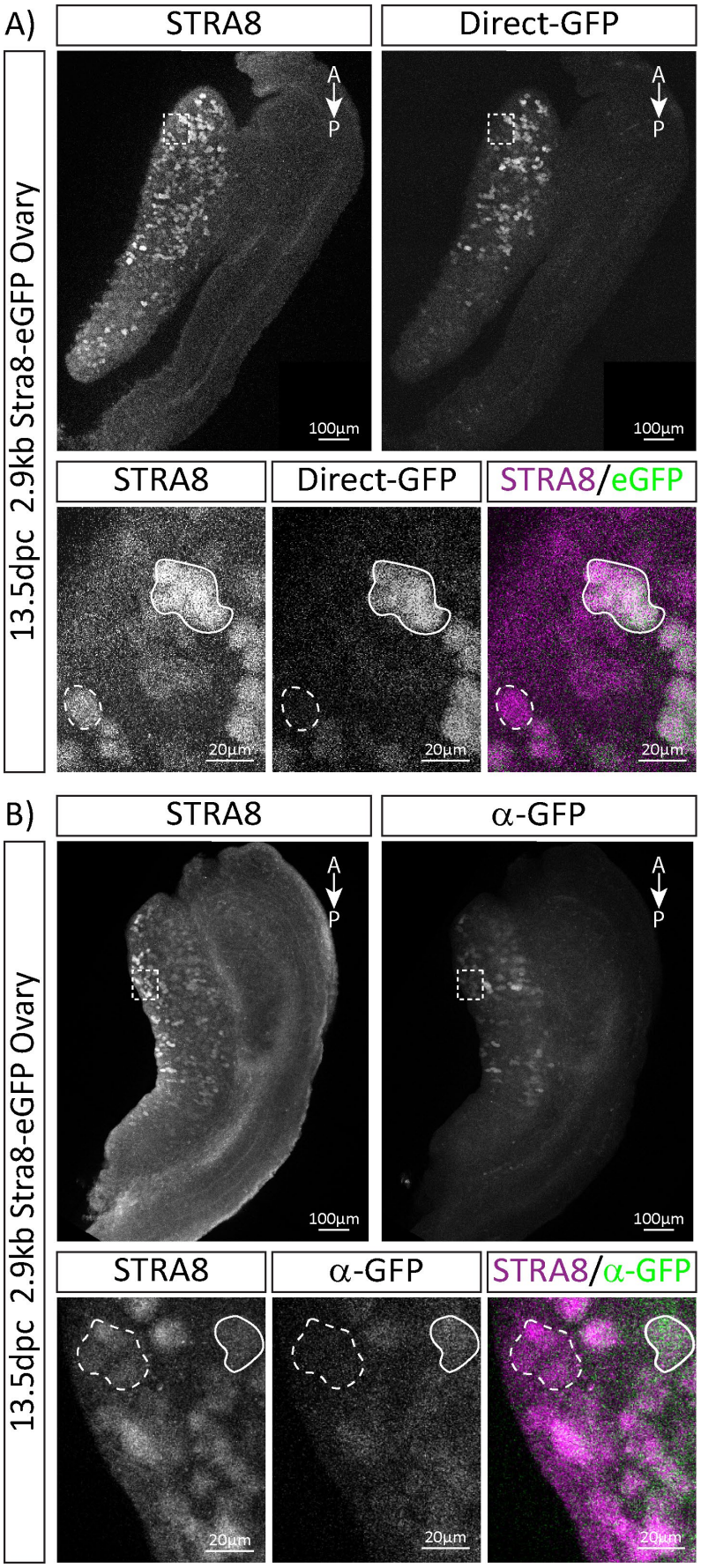

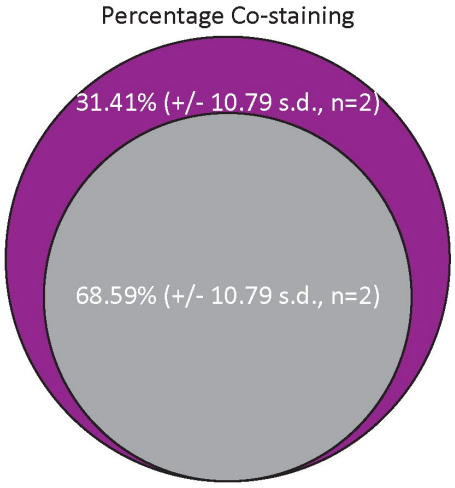

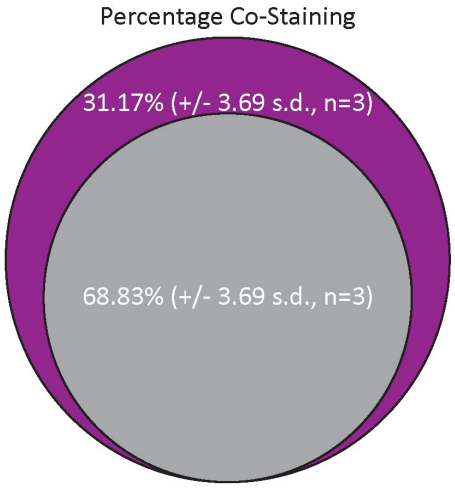

Figure S3: eGFP driven by the 2.9kb *Stra8* promoter co-localises with STRA8 protein expression in approximately 68% of germ cells.

A) Whole mount immunofluoroscence analysis of 13.5 dpc 2.9kb Stra8-eGFP ovaries stained for STRA8 expression, compared to direct eGFP signal produced. Cells co-expressing STRA8/eGFP (solid lined) accounted for 68.59% (+/- 10.79 s.d, n=2, 348 total cells counted) of total STRA8-positive cells (dotted lined). No cells expressing eGFP only were observed. B) Whole mount immunofluoroscence analysis of 13.5 dpc 2.9kb Stra8-eGFP ovaries stained for STRA8 expression, compared to anti-GFP antibody detection. Cells co-staining for STRA8/anti-GFP (solid lined) accounted for 68.83% (+/- 3.69 s.d, n=3, 653 total cells counted) of total STRA8-positive cells (dotted lined). No cells staining for GFP only were observed.

Figure S4

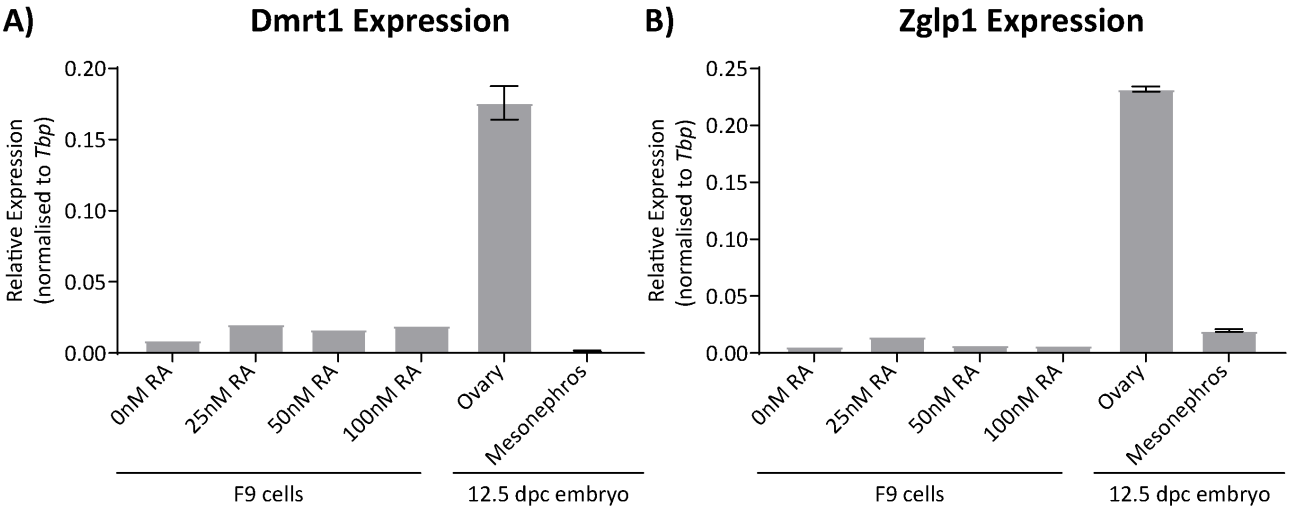

Figure S4: Lack of *Dmrt1* and *Zglp1* expression in F9 EC cells

A) *Dmrt1* is not present at appreciable levels in F9 cells and is not upregulated in response to RA, excluding a mechanism by which RA induces *Dmrt1* expression and DMRT1 drives *Stra8* expression (n = 1, see text for more detail). B) Downstream effector of BMP signalling, *Zglp1,* is not expressed in F9 cells and is not upregulated in response to RA treatment (n=1). Quantitation of expression in 12.5 dpc ovaries and mesonephros are included as positive and negative controls, respectively, for comparison (n=3).

Figure S5

Figure S5: CRISPR/Cas9 mutation strategy of RARE1 and RARE3.

A) RARE1 specific CRISPR guide RNA (RARE1sgRNA) was designed to target RARE1 (black rectangle) at -200nt relative to *Stra8* TSS. Mutataions to RARE1 are incorporated when the CRISPR/Cas9 mediated double stranded break is repaired by homology directed repair (HDR) using co-injected RARE1_ssODN as the repair template. Target sequence was mutated to also disrupt the PAM recognition sequence, to prevent CRISPR/Cas9 re-targeting of successful HDR events. We included a *SalI* restriction enzyme site to facilitate genotyping. B) RARE3 at -1613nt was targeted for mutation using a similar strategy as for RARE1. C) An unplanned non-homologous end joining repair by-product of targeting RARE1 generated the mutant line Δ173bp, where sequence between -55 and -228nt upstream of *Stra8* TSS (encompasing RARE1 and DMRT1 binding sites) was deleted.

Previously identifed RARE2 and a TATA-box like sequence remained intact. The Δ173bp is effectively a *Stra8*-null mouse line as both sexes are infertile.

Figure S6

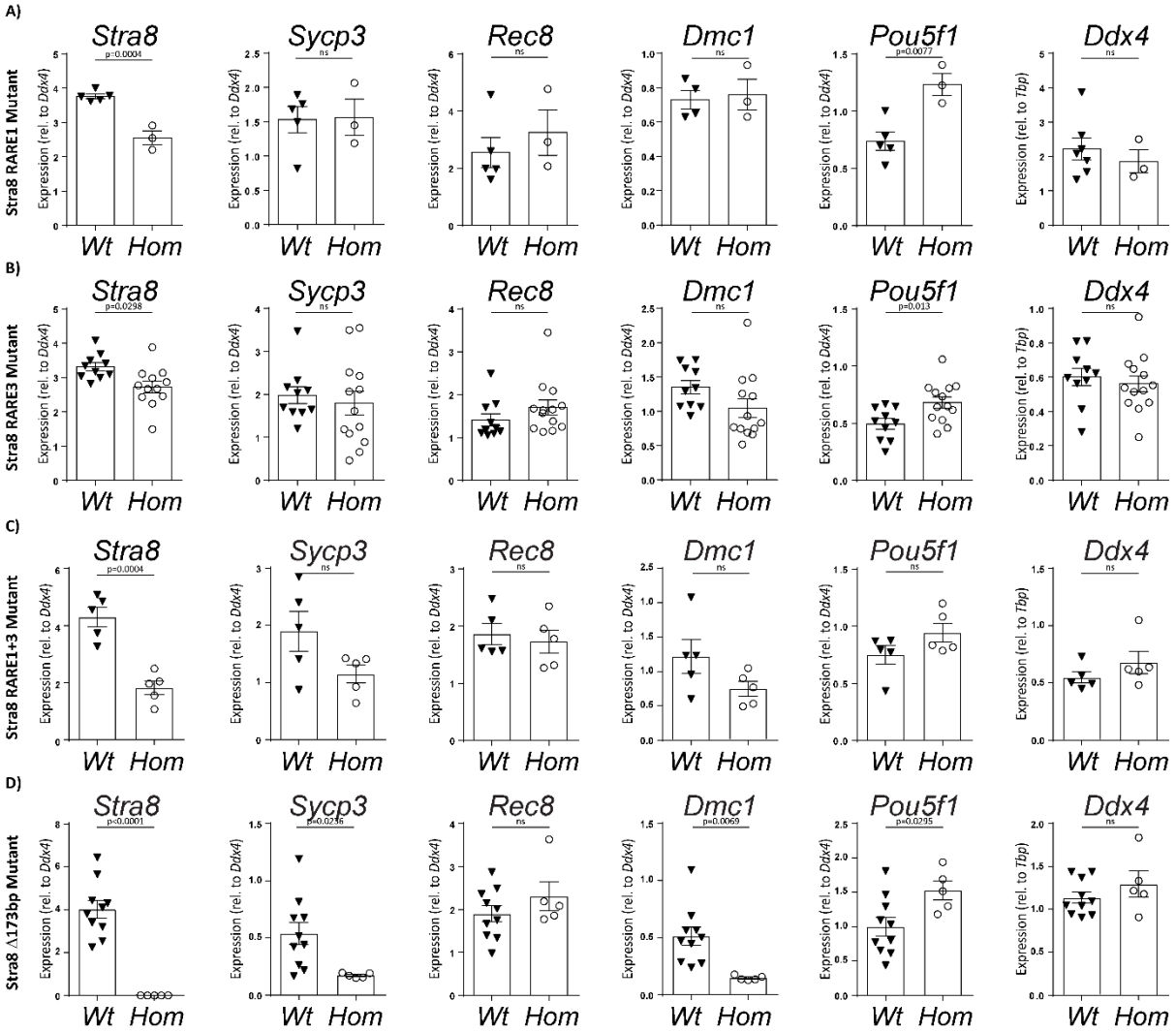

Figure S6: Meiotic and germ cell gene expression in 14.5 dpc fetal ovaries of the CRISPR/Cas9 mutant mouse lines compared to wildtype littermates.

A-C) RARE1, RARE3 and RARE1/3 mutant lines all show decreased *Stra8* expression by qRT-PCR, however other meiotic markers are not significantly perturbed. Importantly *Rec8*, another RA reponsive gene, is unaffected indicating the decrease in *Stra8* expression is not due to lower levels of RA. Retention of *Pou5f1* expression is observed at varying degrees of magnitude. D) In the Δ173bp mutant there is no detectable expression of *Stra8* and expression of later stage meiotic markers *Sycp3* and *Dmc1* is substantially diminished. *Rec8* expression is not significantly altered in RARE1, RARE3 or RARE1/3 lines, as expected (mean ± s.e.m, t-test, n > 3).

Figure S7

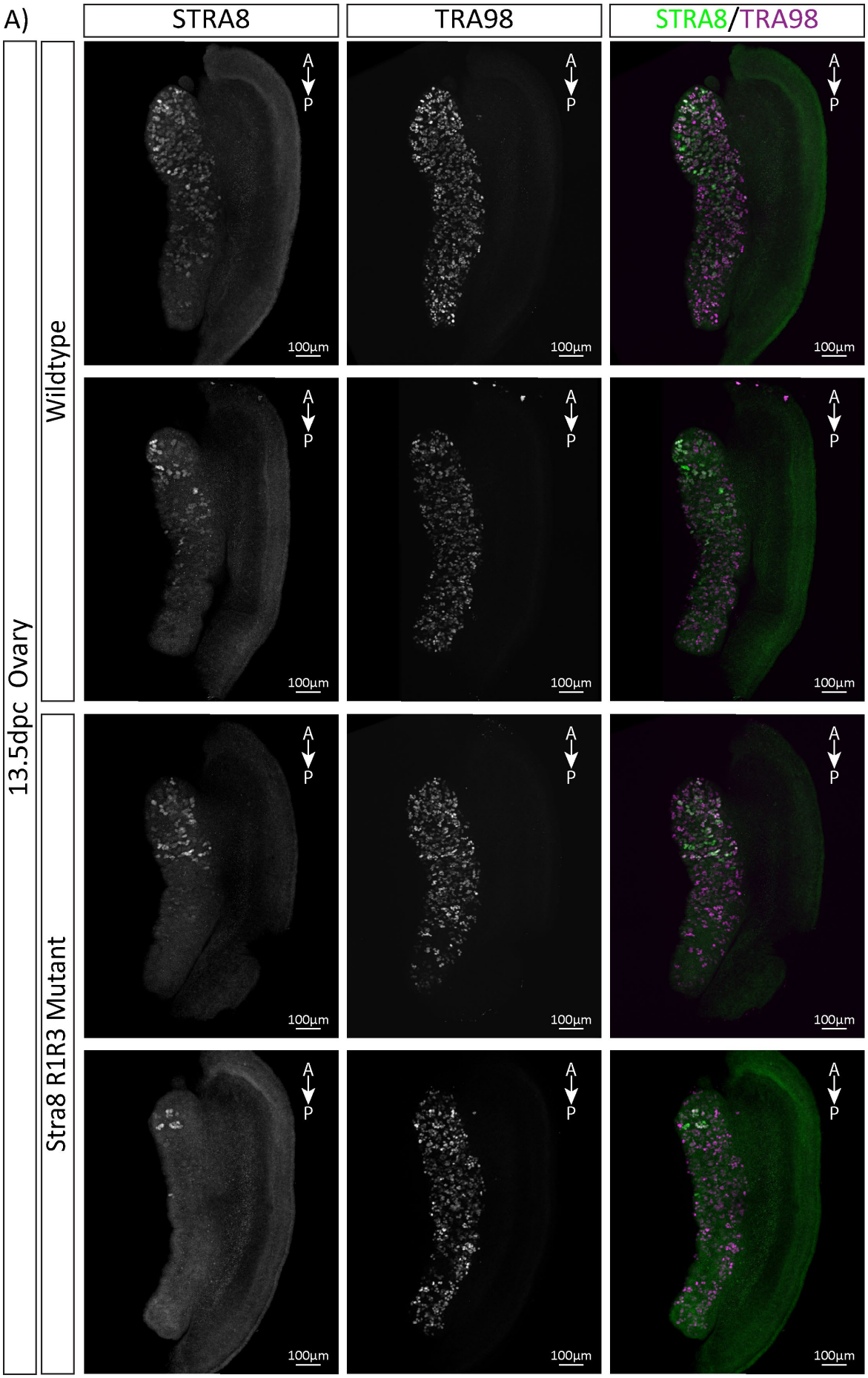

Figure S7: RARE1/3 double mutant retains anterior to posterior wave of STRA8 expression.

Two representative images of whole mount immunofluorescence for STRA8 shows that the anterior to posterior pattern of STRA8 expression see in wildtype ovaries (upper panels) is maintained in RARE1/3 double mutant (lower panels).

Figure S8

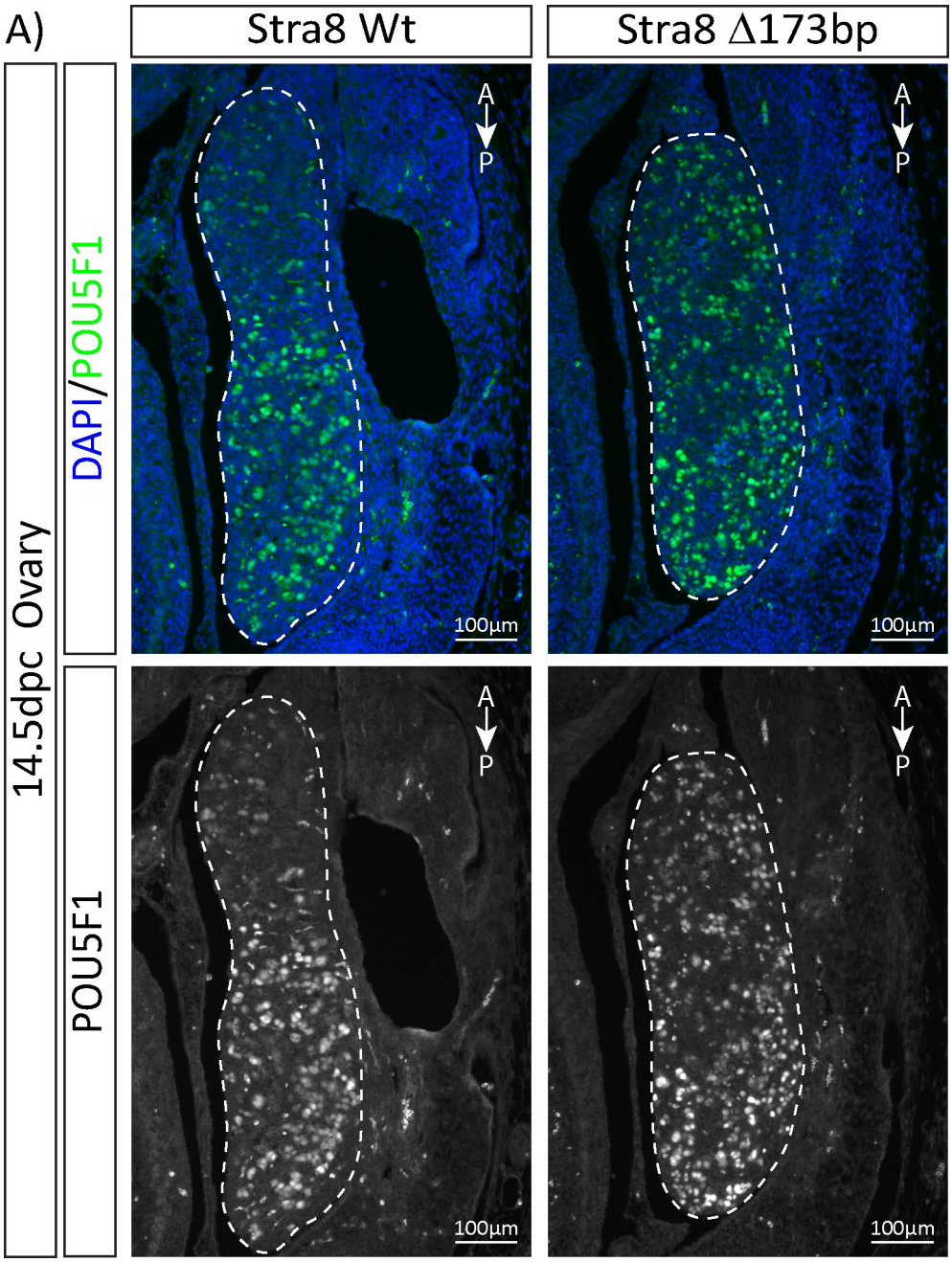

Figure S8: Retention of POU5F1 (a.k.a. OCT4) in Δ173bp mutant ovaries.

Whole mount immunofluoroscence analysis shows the depletion of POU5F1 characteristic at the anterior end of wildtype 14.5 dpc ovaries. This was not observed in a homozygous Δ173bp littermate, where POU5F1 expression is maintained along the entire length of the ovary. This correlates with the retention of *Pou5f1* expression detected by qRT-PCR (Fig. 5B; Fig. S6D).

Figure S9

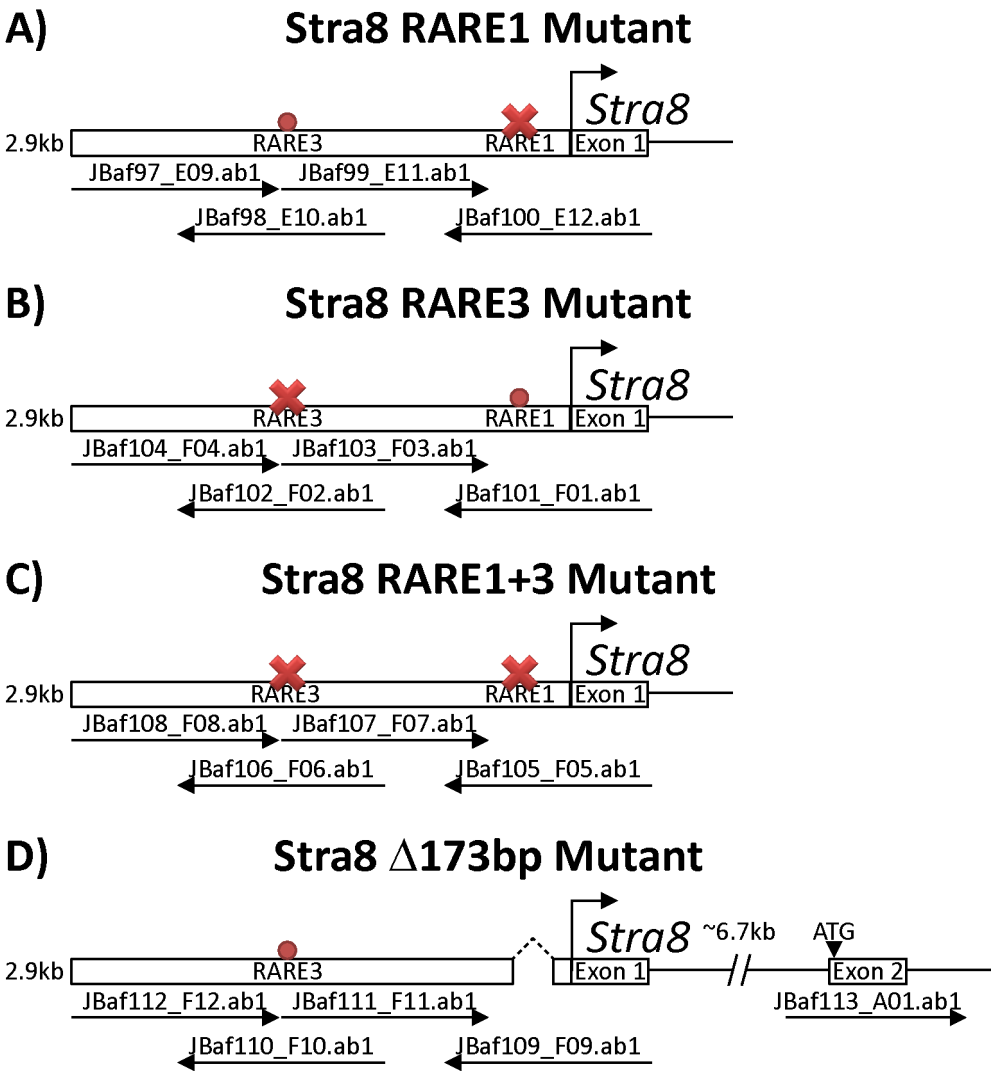

Figure S9: Sequencing coverage of RARE1, RARE3, RARE1+3 and Δ173bp mutant alleles

A-C) 2.9kb promoter and Exon 1 of RARE1, RARE3 and RARE1+3 was cloned and completely sequenced, confirming that only the intended RAREs were mutated. Full overlapping coverage was achieved using 4 primers; reads are as indicated by the black arrows under the diagram of each promoter. D) In addition to sequencing the promoter and Exon 1, the entirety of Exon 2 and flanking intronic sequences were also sequenced for the Δ173bp allele. Exon 2 contains the ATG transcription start site. We confirmed exon 2 to be mutation free, suggesting that it is unlikely that a null allele was inadvertently generated by mutation at that position. All sequencing chromatograms are avaliable as Data S1 (https://doi.org/10.6084/m9.figshare.13506966.v1).

Supplementary Tables

Table S1: Sequences of oligonucleotides used for PCR amplification of genetic sequences, genotyping and SYBR-based qRT-PCR.

Name	Sequence	Used For
2.9kbStra8_F	TCTCGAGCCTTTAGACCCCAGAGC	Amplification of ~2.9 kb *Stra8* promoter
Stra8_R	GACTGCCCGTCGCAGAATAAGAAG	
Stra8_Fw2	TGATTGGTTCGCAGCCTGGG	Genotyping for Stra8-eGFP Transgene
eGFP_Rv1	CGTCGCCGTCCAGCTCGACCAG	
Col1a1-Geno7	CCCAGCTTCACCAGTTCAAT	Genotyping for *Col1a1* Targeting
Col1a1-Geno8	TCATCAAGGAAACCCTGGAC	
GFP_F	GCAGAAGAACGGCATCAAGGTG	GFP qRT-PCR Primers
GFP_R	CTGGGTGCTCAGGTAGTGGTTGTC	
DDX4_F	CAGGAATGCCATCAAAGGAACAAC	DDX4 qRT-PCR Primers
DDX4_R	CCCAACAGCGACAAACAAGTAACTG	

Table S2: Oligonucleotides sequences used for site directed mutagenesis of RARE1, RARE3 and DMRT1 binding sites on *Stra8* promoter constructs for *in vitro* luciferase assays.

Name	Oligo Sequence	Used For
RARE1_ssODN	GCTCCTCTATATCTCAAGAGAAAG TTATAGGTGGCATTGCCCTGGTTG AGGGGTGTAAGAACTGGCGCTAGC CGCCTGGATGGTCGACAAAATTTT TCTTGCTCCTTCCACACCCTCTTGC AACCTGTGGCAAGTTGTTACAATG TTTTCACCAATGTCCACGCTCCCCA TTGGCGCCCCACCATG	Mutation of RARE1 binding site (mutated nucleotides are underlined) RARE1 GGGTGAAAAGGTCA Mutated GTCGACAAAATTTT
Stra8_mutRARE3_antisense	CTTTGTCTTGGAGAGCCTTGTCCTG TCGACAAATTTAATGTGGAGGTTT GCAAACTTTG	Mutation of RARE3 binding site (mutated nucleotides are underlined) RARE3 TCCTCACAGGTCA Mutated TAAATTTGTCGAC
Stra8_mutDMRT1_antisense	GGCGCCAATGGGGAGCGTGGACAT TGGTGAGGCGCGCCGGATCCCTTG CCACAGGTTGC	Mutation of DMRT1 binding site (mutated nucleotides are underlined) DMRT1 TTGTTACAATGTTTT Mutated GGATCCGGCGCGCCT

Table S3: Oligonucleotides sequences used for the generation of CRISPR/Cas9 reagents to target mutations of RARE1 and RARE3 *in vivo*.

Name	Oligo Sequence	Used For
RARE1 -top	CACCGGCGCTAGCCGCCTGGAT	Annealed and inserted into PX330 to generate RARE1 sgRNA template for IVT
RARE1 -bottom	AAACATCCAGGCGGCTAGCGCC	
RARE1_ssODN	GCTCCTCTATATCTCAAGAGAAAG TTATAGGTGGCATTGCCCTGGTTG AGGGGTGTAAGAACTGGCGCTAGC CGCCTGGATGGTCGACAAAATTTT TCTTGCTCCTTCCACACCCTCTTGC AACCTGTGGCAAGTTGTTACAATG TTTTCACCAATGTCCACGCTCCCCA TTGGCGCCCCACCATG	HDR template for generating CRISPR/Cas9 mediated RARE1 mutation
RARE3_sgRNAF	AATACGACTCACTATAGGGGCAAA CCTCCACATTCCTCACGTTTTAGAG CTAGAAATAGCAAGTTAAAATAAG GCTAGTC	Annealed and filled to generate template for RARE3 sgRNA IVT.
Chimeric_sgRNA_R	TAAAAAAGCACCGACTCGGTGCCA CTTTTTCAAGTTGATAACGGACTA GCCTTATTTTAACTTGCTATTTCTA GCTCTAAAAC	
RARE3_ssODN	ACTAAATTAAAGGCTGAGACCTGT CAGAGGTCAAAGTTTGCAAACCTC CACATTAAATTTGTCGACAGGACA AGGCTCTCCAAGACAAAGGTTCAC AGTTTCAGTACCCGTTCTGCACCC	HDR template for generating CRISPR/Cas9 mediated RARE3 mutation

Table S4: Breeding Statistics for Δ173 heterozygous and homozygous mice

Number of breeders	Average Days Setup (S.D.)	Average Days to birth of 1st litter (S.D.)	Average number of litters (S.D.)	Average litter size (S.D.)
16 Heterozygous (11M, 5F)	173.55 (87.75)*	29.45 (12.81)	4.36 (2.31)	7.11 (1.52)
8 Homozygous (4M, 4F)	82.75 (5.02)	N/A	0	0

*Statistics extracted from breeding colony: breeders were allowed to breed for longer than was done for the homozygous animals. S.D. = standard deviation.